

# Hawaii National Marine Renewable Energy Center (HINMREC)

U.S. Department of Energy Award Number:  
DE-FG36-08GO18180

## Task 6: Supporting Studies

# OTEC Heat Exchanger Program: 2015 Ultrasonic Scanning for Corrosion Monitoring Report

Prepared by:  
Makai Ocean Engineering

Prepared for:  
Hawaii Natural Energy Institute, University of Hawaii

February 2015



**OTEC HEAT EXCHANGER PROGRAM**  
**ULTRASONIC SCANNING FOR CORROSION**  
**MONITORING**

**FINAL REPORT**

**SUBAWARD MA140003**

Prepared For

**HAWAII NATIONAL MARINE RENEWABLE ENERGY CENTER**

**LUIS VEGA**

1680 East West Road, POST 112A

Honolulu, HI, 96822

USA

Prepared By

**MAKAI OCEAN ENGINEERING**

PO Box 1206, Kailua, Hawaii 96734

February 10, 2015

(Version 2)

# 1. SUMMARY

Seawater corrosion of aluminum alloys can adversely impact the lifetime and performance of aluminum Ocean Thermal Energy Conversion (OTEC) heat exchangers. Since uniform corrosion rates for the aluminum alloys being considered for use in OTEC heat exchangers are low, the primary corrosion mechanisms of concern are surface pitting and crevice corrosion at gasket interfaces. Makai Ocean Engineering has developed a system to observe pit growth in-situ using optical imaging and ultrasonic thickness measurements which allows corrosion development to be monitored over time without the removal and destruction of samples. Three aluminum alloys were chosen for testing (Al 2024, Al 6061-T651 and Al 5086-H116) in flowing (1 m/s) and near-stagnant cold, deep seawater (6 samples total) provided by the National Energy Laboratory of Hawaii Authority in Kailua-Kona, Hawaii.

Al 2024 and Al 6061 samples began to corrode shortly after exposure to seawater; corrosion product appeared on the surfaces after 3 and 20 days respectively. For these alloys, the maximum pit depths in flowing and near-stagnant seawater sources were similar. After 4.5 months of exposure, the maximum pit depths of the Al 2024 and Al 6061 samples were 0.8 mm and 1.2 mm respectively. Initially, the maximum pit depth of the Al 2024 and Al 6061 samples increased linearly with time. After 12 weeks, the maximum pit depth of the Al 2024 samples leveled off while the maximum pit depth in the Al 6061 samples continued to increase linearly. The increase in corroded surface area and volume followed the same trends as the increase in maximum pit depth. After 4.5 months, 10-50% of Al 2024 and Al 6061 sample surfaces were covered by corrosion product; the extent of coverage would alter the flow and heat transfer performance of heat exchangers made from these alloys. Corrosion has been detected at the gasket interface of the Al 5086 sample in near-stagnant seawater but no corrosion has been observed on Al 5086 in flowing seawater.

In all corroding samples, the ultrasonic scans revealed crevice corrosion progressing underneath the gasket interface. The largest amount of gasket corrosion occurred in the near-stagnant water conditions. Maximum pit depths of 0.8 mm underneath the gasket and lateral penetrations of 6 mm from the inside edge of the gasket have been observed. For Al 5086 and Al 6061, a significant change in open circuit potential (measured against an Ag/AgCl reference electrode) was observed at the onset of corrosion.

We discuss the implications of aluminum corrosion on OTEC heat exchangers and offer techniques to implement corrosion monitoring in an OTEC plant.

## 2. INTRODUCTION

Aluminum alloys have been proposed for use in OTEC heat exchangers for their high thermal conductivity, comparatively low cost, and overall good general corrosion resistance (due to formation of a protective oxide layer) in seawater environments. Although uniform corrosion rates for aluminum alloys are low, aluminum alloys are susceptible to surface pitting and crevice corrosion at gasket interfaces which can initiate when local galvanic cells develop between alloying elements and deposit corrosion product on the surface of the metal. The corrosion product encases the immediate area and changes the local environment which acts to accelerate the corrosion process. It is important to quantify this phenomenon because in time, corrosion can penetrate the wall of the heat exchanger and allow refrigerant to leak into the seawater. For heat exchangers, this is considered a catastrophic failure and must be avoided.

Makai Ocean Engineering has been studying and quantifying the deployment of corrosion on many alloys being considered for OTEC heat exchangers. While important results have been obtained from previous experiments, samples had to be removed and processed to remove the corrosion product buildup prior to obtaining quantitative measurements. Measurements of pit sizes, numbers, and depths over time were compiled from several different samples of the same alloy.

Makai Ocean Engineering has developed a setup to observe pit growth in-situ using optical imaging and ultrasonic scanning. With imagery, pitting sites can be identified and the buildup of corrosion product on the metal's surface can be observed over time. However, once corrosion product encapsulates a pit, no accurate measurements of pit size or depth can be made via imaging alone. However, the surface underneath the corrosion product can be observed using ultrasonic thickness measurement from of the back side of sample. Ultrasonic scanning enables the development of pitting and crevice corrosion to be monitored over time without removal or destruction of samples. Parameters such as maximum pit depth, pitted surface area, pitted volume, and corrosion buildup area can be quantified using imaging and ultrasonic measurements and extrapolated to estimate heat exchanger lifetime and changes in performance.

### 3. TEST PLAN

Imaging and ultrasonic thickness measurements were used to observe samples of three different aluminum alloys placed in cold, deep seawater (Table 1) supplied to Makai’s Ocean Energy Research Center (OERC) by the National Energy Lab of Hawaii Authority (NELHA) located at Keahole Point in Kailua-Kona, Hawaii. Localized corrosion of aluminum in deep seawater is more severe than in surface seawater; therefore, testing was conducted in cold seawater source. The goal of the study is to measure pit growth and concentration over time and to characterize crevice corrosion that occurs at gasket interfaces.

<b>Depth</b>	674 m
<b>Temperature</b>	6.6 °C
<b>Salinity</b>	34.2 PSU
<b>Dissolved Oxygen</b>	1.3 ppm
<b>pH</b>	7.6

*Table 1: Average deep-seawater properties at NELHA.*

Three aluminum alloys were tested: two alloys that are being considered for OTEC shell-and-tube heat exchangers (Al 6061 and Al 5086) and a quickly corroding alloy (Al 2024) used to refine our experimental technique and analysis (Table 2). Material certifications were obtained for the Al 5086 and Al 6061 samples but not for Al 2024. One sample of each alloy was exposed to seawater flowing at 1 m/s, which is representative of the actual flow in a heat exchanger. Since areas of dead flow are unavoidable in a heat exchanger (e.g., at gasket interfaces) a second sample of each alloy was placed in near-stagnant water.

<b>Alloy</b>	<b>Temper</b>	<b>Si (%)</b>	<b>Fe (%)</b>	<b>Mn (%)</b>	<b>Mg (%)</b>	<b>Cu (%)</b>	<b>Ti (%)</b>	<b>Cr (%)</b>	<b>Zn (%)</b>
Al 6061	T651	0.65	0.39	0.06	1.00	0.29	0.016	0.067	0.017
Al 5086	H116	0.125	0.308	0.450	4.495	0.055	0.008	0.065	0.117
Al 2024	unknown	< 0.5	< 0.5	0.3 - 0.9	1.2 - 1.8	3.8 - 4.9	< 0.15	< 0.1	< 0.25

*Table 2: Elemental composition of alloys tested.*

The samples were mounted such that one side was exposed to seawater and the other side open for ultrasonic measurements. Samples were imaged on a daily basis, and ultrasonic scans of all the samples were performed at least weekly. Open circuit potentials of the samples versus a standard Ag/AgCl reference electrode were also recorded.

## 4. APPARATUS

The testing apparatus consisted of three components: imaging racks used to expose the samples to seawater flow, take daily images, and take open circuit potential measurements; ultrasonic thickness scanning equipment; and a laser profilometer to measure a sample's surface features before and after being exposed to seawater.

### 4.1. CORROSION IMAGING RACKS

Makai Ocean Engineering has been using a custom designed multi-column imaging racks (MCIR) to expose metal samples to seawater (Figure 1). The acrylic windows enable real-time, in-situ observation of surface changes. Computer controlled cameras mounted on a motorized X-Y-Z stage take daily images of all samples. Both low (70 mm x 50 mm FOV, 27  $\mu\text{m}$  pixels) and high (1 mm x 0.8 mm FOV, 0.4  $\mu\text{m}$  pixels) magnification cameras are used. For each sample, low magnification images of the entire surface are recorded and smaller regions of interest are imaged at higher magnification.



*Figure 1: Multi-column imaging racks used to expose samples to seawater flow. Seawater flows from the top of the columns. Cameras are mounted on an X-Y-Z stage and programmed to take daily images of sample surfaces.*

For this study, two of the MCIR columns were modified so three samples (one of each alloy) could be mounted in a single column with their backside of the sample accessible to the ultrasonic thickness scanner (Figure 2). Samples were placed in slightly indented frames and sealed with face gaskets made of silicone rubber at a compression of 20% (Figure 3).



*Figure 2: Left – modified columns with multiple samples exposed to seawater. Right – the back of the samples where ultrasonic thickness measurements are taken.*

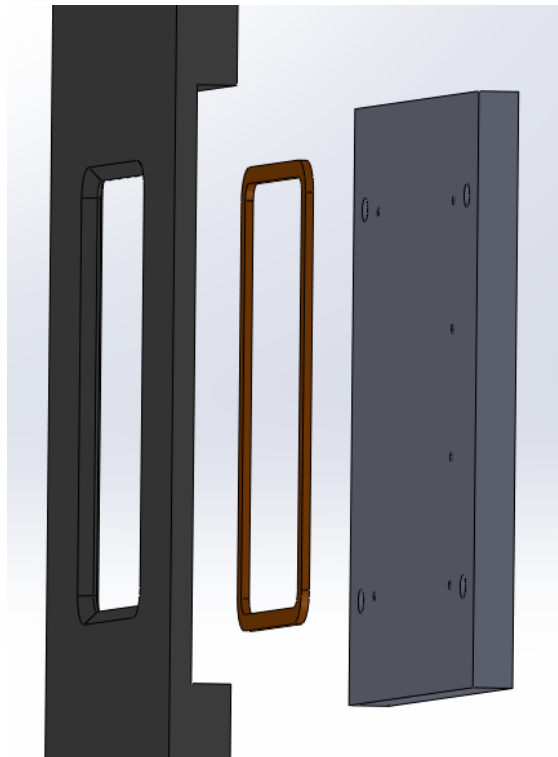


*Figure 3: Explosion view of the mounting frame, gasket and corrosion sample*

Sample surfaces have light tool marks from the machining process. Care was taken during machining to prevent metal shavings or other contaminants from contacting sample surfaces. Holes of various depths (Figure 4) placed in each sample were used as calibration and reference points to align the ultrasonic scans to the optical images. The holes lie outside of the gasketed area and are not exposed to seawater flow. Prior to mounting, the samples were cleaned with Simple Green™ and rinsed with methanol.

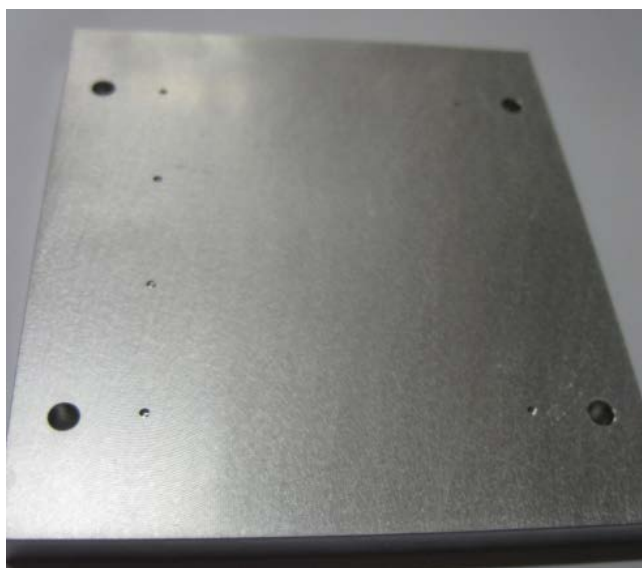


*Figure 4: Sample face prior to exposure to water. Small holes of various depths were added outside the flow area for calibration and to align the ultrasonic scans and optical images.*

#### 4.2. ULTRASONIC THICKNESS SCANNER

An ultrasonic scanner manufactured by NDT Systems which integrates a Raptor© Imaging Flaw Detector with a 13 mm diameter 15 MHz ultrasonic transducer was used in this study. The ultrasonic thickness scanner sends a high-frequency sound pulse from the transducer placed on one side of a sample. The time it takes for the reflected pulse to return from the far side of the sample is a measure of the sample's thickness. A fresh water source is provided to the face of the transducer as a sonic couplant and also functions as a lubricant. Thickness measurements across the sample were obtained with an NDT System's Tunnelscan© motorized X-Y stage with a 300 mm x 450 mm scan area. An X-Y stage allows a 3-dimensional surface to be created from individual thickness measurements. Mounting this stage to the back of the imaging racks permitted monitoring of several corrosion coupons with one setup (Figure 5).

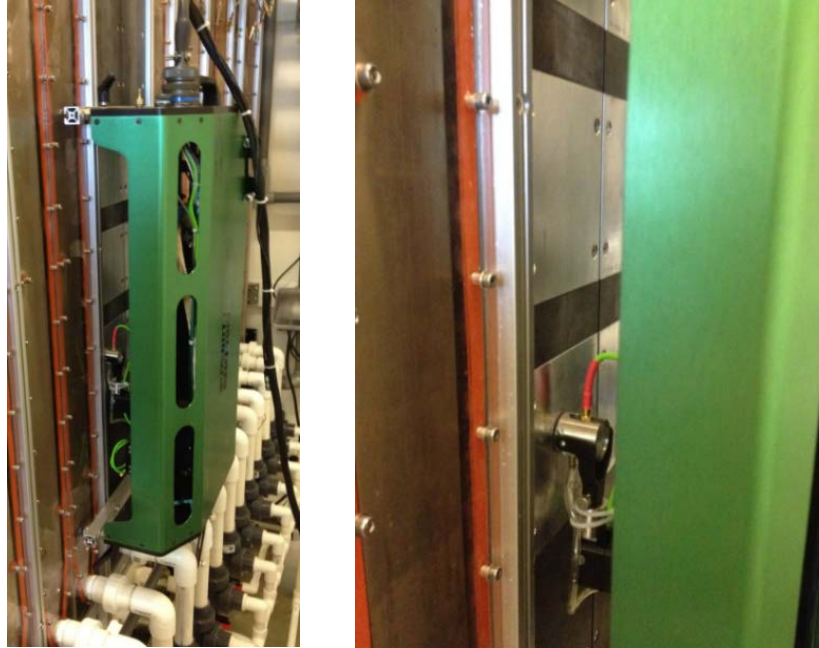


*Figure 5: Left - Scanning stage mounted to the back side of the imaging racks. Right - Ultrasonic transducer in contact with sample.*

Ultrasonic scans are not precisely repeatable measurements due to noise and other effects. In some cases ‘streaky’ scans caused by poor transducer contact prevented good measurements. In addition, some scans may have slightly different depth measurements due to variations in transducer contact, so sudden decreases in pit depth observed from one scan to the next are spurious. This variability can lead to errors of approximately 40  $\mu\text{m}$  in pit depth measurements.

#### 4.3. LASER PROFILOMETER

A CCS Prima® manufactured by Nanovea and a custom built motorized X-Y stage (Figure 6) was used to create three-dimensional profiles of a sample surface. The laser profilometer uses chromatic confocal measurements to determine the distance to a surface from the laser head. The laser profiles can only be obtained prior to seawater exposure and after the sample is removed from seawater and corrosion product cleaned from its surface. The profilometer has high lateral and depth resolution, 8  $\mu\text{m}$  and 1  $\mu\text{m}$  respectively.



*Figure 6: The laser profilometer scans the surface of a sample to measure corrosion depths.*

#### 4.4. COMPARISON OF MEASUREMENT TECHNIQUES

There are advantages and disadvantages to each of three different measurement techniques. The major drawback of the ultrasonic measurements is the large beam size of the transducer (13mm) makes pits look larger. Figure 7 compares ultrasonic and laser profilometer measurements of a pre-drilled flat-bottomed reference hole. Despite the difference in measured feature size, both techniques yield a consistent depth for the pre-drilled hole.

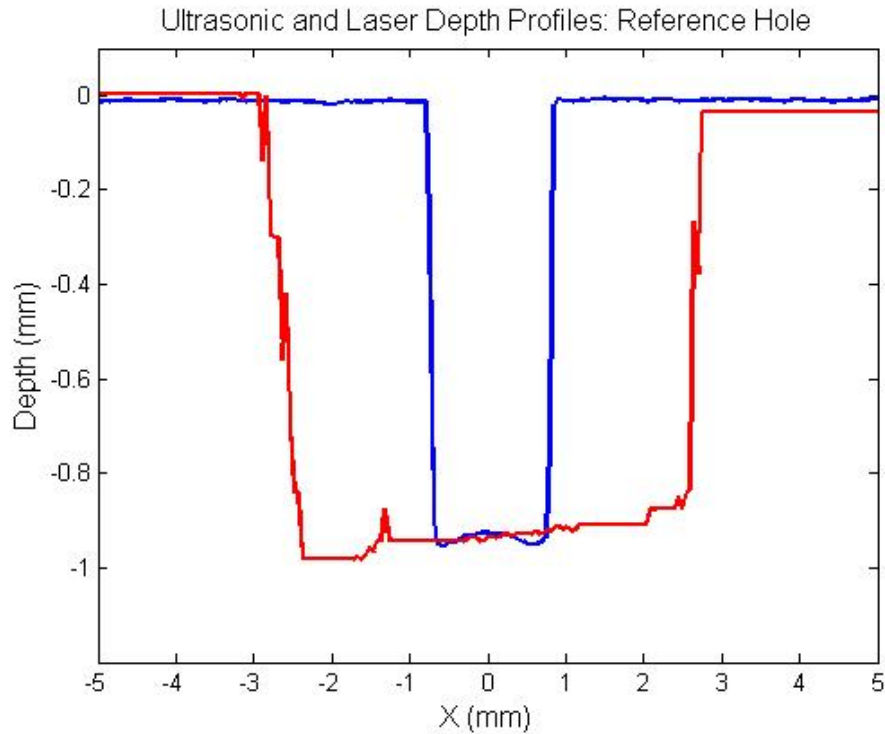


*Figure 7: Comparison of a 0.76 mm diameter reference-hole profile measured ultrasonically (red) and with the laser profilometer (blue).*

Ultrasonic measurements are ideal for in-situ measurements of heat exchanger wall penetration due to corrosion. This method can be implemented on an OTEC plant without disturbing operation. The maximum pit depth observed by the scanning will be instrumental in estimating lifetimes of OTEC heat exchangers.

The higher resolution laser profilometry helps us understand the mechanisms at work in the corrosion process. However, laser profilometry cannot be performed on heat exchangers without component removal.

Although imaging is non-destructive it is not easily implemented because it requires windows to view the interior surfaces of the heat exchanger or highly specialized imaging systems. Imaging is useful from an experimental point of view, correlations can be drawn between surface behavior and pit depth. Studying the build-up of corrosion product over time or as a function of pit depth allows us to estimate the loss of heat exchanger efficiency due to fouling by corrosion product.

Measurement	Type	Lateral Resolution	Depth Resolution	Can be implemented in an operating OTEC plant?
Ultrasonic Scanning	Non-destructive	3 mm	40 $\mu\text{m}$	Yes
Laser Profilometry	Destructive	8 $\mu\text{m}$	1 $\mu\text{m}$	No
Imaging	Non-destructive	27 $\mu\text{m}$ , 0.4 $\mu\text{m}$	none	Difficult

*Table 3: Comparison of measurement techniques.*

## 5. ANALYSIS

The multiple measurement techniques were used to characterize the development of corrosion over time for each alloy. Ultrasonic measurements of pit depth and pitted surface area were used to establish pit growth and crevice corrosion rates which are crucial in establishing the lifetime of an OTEC heat exchanger. To separate the effect of crevice corrosion, only data from the center of the sample (65% of the total exposed surface area) was used to determine pit depth and coverage. In these regions the maximum pit-depth and area of corrosion deeper than 0.1 mm (pitted area) were measured. The mean corrosion-depths (proportional to the total volume of material removed) was calculated from the pit-depth and pitted area measurements. Because area and volume measurements determined by the ultrasonic scans are biased due to the large beam size, the values were normalized by comparing them to the final laser-profilometer scans. Although the scaling is not precise, it provides a reasonable measure of sample's overall corrosion development.

The surface area covered by the white gelatinous corrosion product was measured from the daily images. This parameter is correlated the loss of effective heat-transfer area, and thus, reduction of heat exchanger performance over time.

Three samples were removed for laser profilometer analysis. Both Al 2024 samples and Al 6061 sample from the near-stagnant water source were severely corroded and removed because little value could be obtained from continued testing. Corrosion product was removed with nitric acid in accordance with ASME G1-03. Once clean, the sample surfaces were scanned with the profilometer at 25  $\mu\text{m}$  resolution and compared with corresponding ultrasonic and imaging data. A final ultrasonic scan was performed after corrosion product removal to confirm that the presence of corrosion product has negligible influence in the depths measured ultrasonically.

## 6. RESULTS

Corrosion samples have been exposed to flowing (1 m/s) and near-stagnant cold, deep seawater for 4.5 months. Imaging, ultrasonic thickness measurements, and electro-chemical monitoring have been performed on a weekly (or more frequent) basis.

### 6.1. OBSERVATIONS

The latest images and ultrasonic scans are shown below (Figures 8 and 9). Time lapses of each sample are shown in Appendixes A-E.

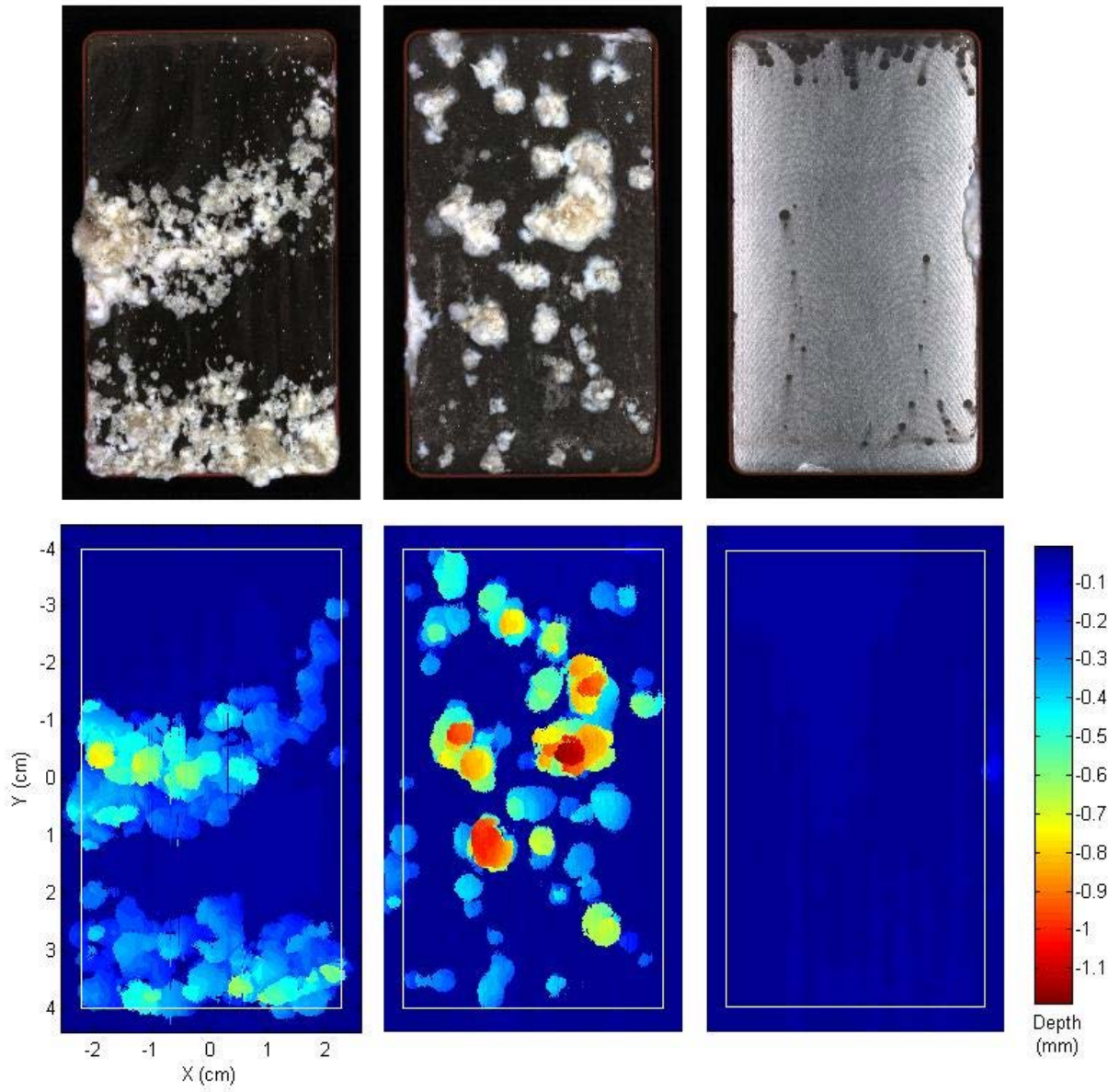


*Figure 8: Images (top) and corrosion depths measured by ultrasonic scanning (bottom) after 150 days in near-stagnant, cold seawater (left - Al 2024, middle - Al 6061, left - Al 5086). White box on ultrasonic images is the location of the gasket.*

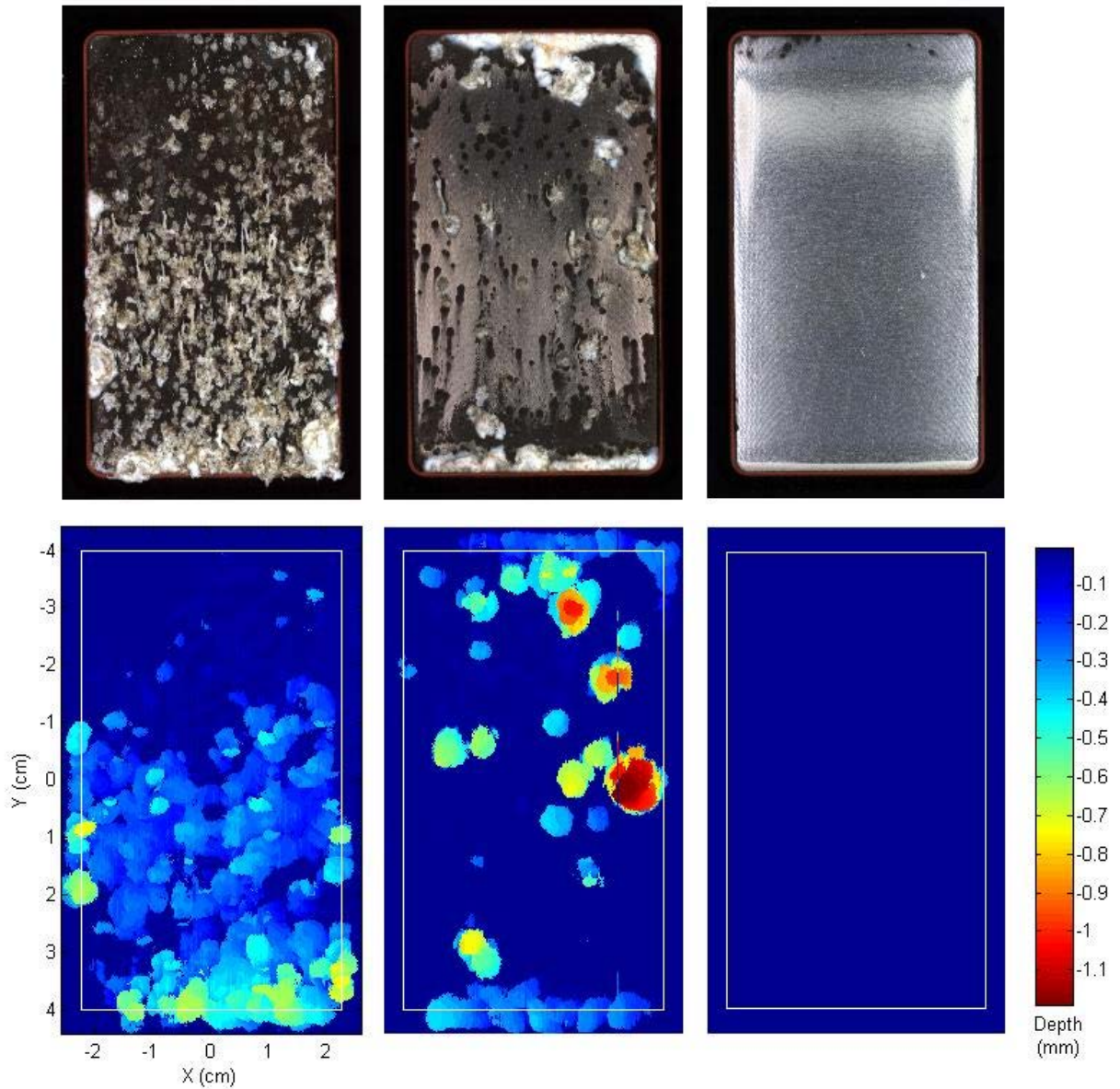


*Figure 9: Images (top) and corrosion depths measured by ultrasonic scanning (bottom) after 150 days in 1 m/s flowing cold seawater (left - Al 2024, middle - Al 6061, left - Al 5086). White box on ultrasonic images is the location of the gasket.*

Al 2024 was chosen as a test alloy because of its high copper content which accelerates corrosion due to galvanic action. Although this alloy is not in consideration for OTEC heat exchangers, it was tested to allow us to quickly refine our analysis procedures. Al 2024 was the first to corrode; corrosion product appeared on the surface after 3 days in both near-stagnant and flowing water. Corrosion was detected ultrasonically on both samples one week later. Pitting corrosion and gasket corrosion were the dominant modes of corrosion. The sample surfaces developed a dark-red color over time. Corrosion product build-up was different between the two flow environments; the flowing seawater sample had smaller but more numerous accumulations in the center of the sample compared to the near-stagnant seawater sample.

The Al 6061 samples also corroded quickly; corrosion product appeared on the surfaces after 20 days for the near-stagnant and flowing seawater samples. Pitting and gasket corrosion were the primary modes of corrosion. Pits were first detected ultrasonically after 25 and 40 days for the near-stagnant and flowing seawater samples respectively. In stagnant seawater, a dark red background color covered the surface similar to the Al 2024 samples. Corrosion product accumulation was greater and more distinct in the near-stagnant sample relative to the flowing seawater sample. In flowing seawater, the uniform dark red color was not established on the surface; instead, dark spots which are bacterial colonies have taken hold (Figure 10).



*Figure 10: Bacterial colonies growing on the surface. Image is approximately 1 cm x 1 cm.*

Al 5086 has shown the best corrosion resistance of the alloys tested. To date the only indication of corrosion is at the gasket interface on the near-stagnant sample after 55 days. Although the corrosion is barely detectable in the ultrasonic scans (after 125 days), it is progressing underneath the gasket. Bacterial attachment is also occurring on both samples; more has accumulated on the near-stagnant sample because lower flow velocities make it easier for bacteria to attach and establish colonies.

## 6.2. CORROSION PRODUCT COVERAGE

Corrosion product (aluminum oxide) builds up from a sample surface as white gelatinous accumulations. In flowing water ‘stalagmites’ can grow upstream from the pit locations (Figure 11). The accumulation of product can extend many millimeters from the surface. Pieces of the corrosion product occasionally break off and then regrow, especially if a change in flow conditions occurs.



*Figure 11: Left - White corrosion product built up from the surface of the Al 2024 sample in near-stagnant seawater. Right - Corrosion product growing in the upstream direction on the Al 6061 sample in flowing seawater.*

Figure 12 plots the accumulation of corrosion product on the sample surfaces over time. This is an important parameter because corrosion product buildup can restrict flow channels, change local flow regimes, decrease thermal conductivity and ultimately, significantly reduce heat transfer performance of the heat exchanger. If alloys are poorly selected, corrosion product could cover more than 10% of the surface within a few months.

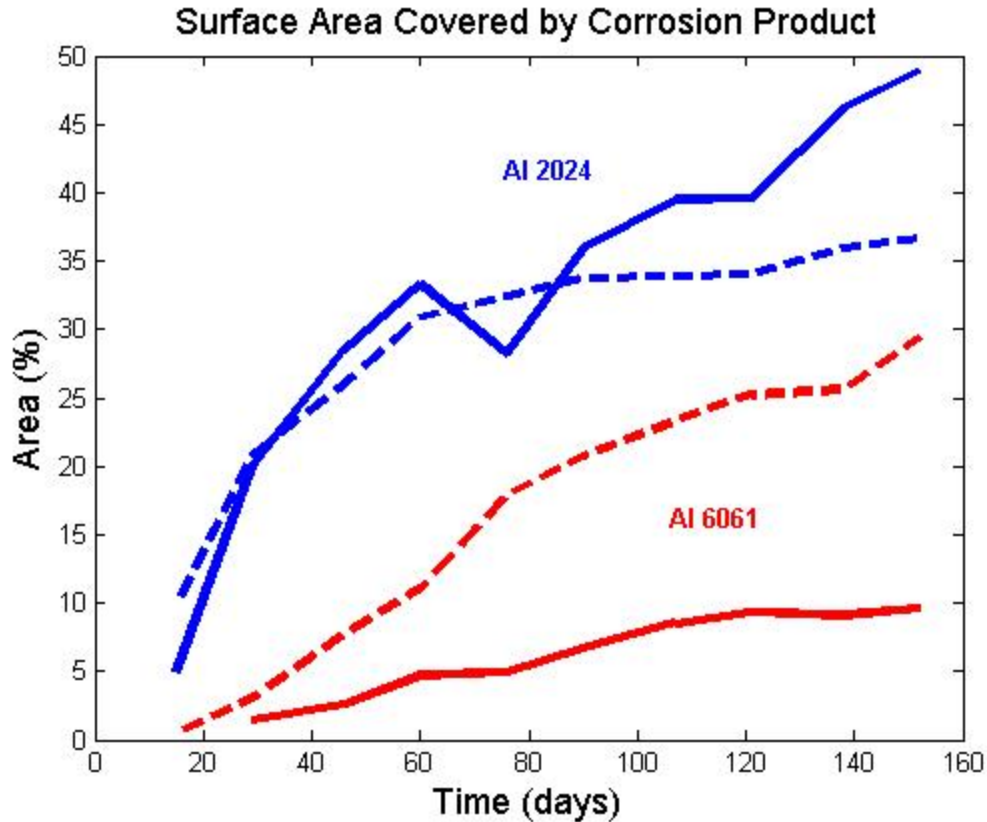


Figure 12: Surface area covered with corrosion product for the two alloys exhibiting pitting corrosion. Dashed lines are samples in near-stagnant seawater, solid lines are in 1 m/s flowing seawater.

### 6.3. MAXIMUM CORROSION DEPTHS

The maximum pit depth is plotted versus time in Figure 13. After a few weeks of rapid pit growth, deepening of pits on Al 2024 samples slowed down. The Al 6061 samples show a nearly uniform rate of corrosion deepening. With pits depths of approximately 1 mm within a few months, a typical shell-and-tube heat exchanger made from Al 2024 or Al 6061 would quickly fail. Al 5086 has so far performed better, only showing signs of corrosion at the gasket in near-stagnant seawater.

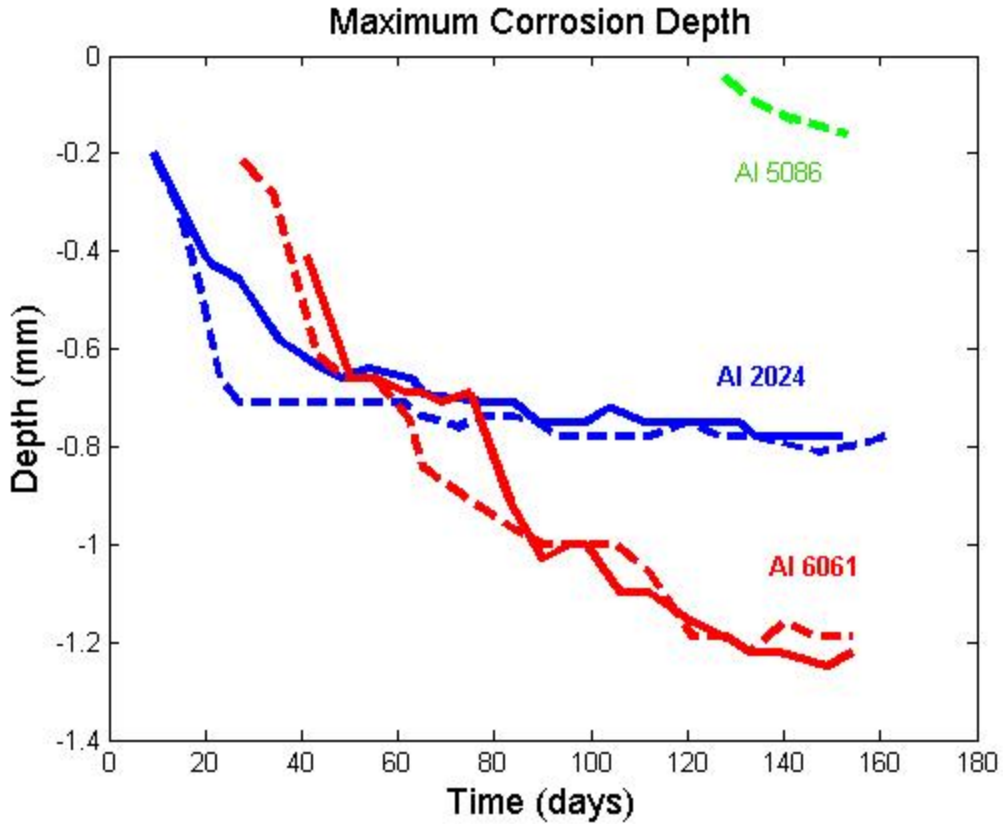


Figure 13: Maximum corrosion depth over time for the alloys showing corrosion. Dashed lines are samples in near-stagnant seawater, solid lines are in 1 m/s flowing seawater.

#### 6.4. CORRODED SURFACE AREA

Another parameter determined from the ultrasonic measurements is the surface area covered by pits (defined as the area with pits depths greater than 0.1 mm). Because the large ultrasonic beam size makes accurate measurement impossible, the results were normalized based on laser profilometer scans of samples that were removed. While the percent area coverage is an estimate, the relative behavior over time is reflective of corrosion development (Figure 14). Increases in the corroded surface area followed the same trend as increases in the maximum pit depth. The rate of increase in corroded surface area slowed over time for Al 2024 but remained constant for Al 6061.

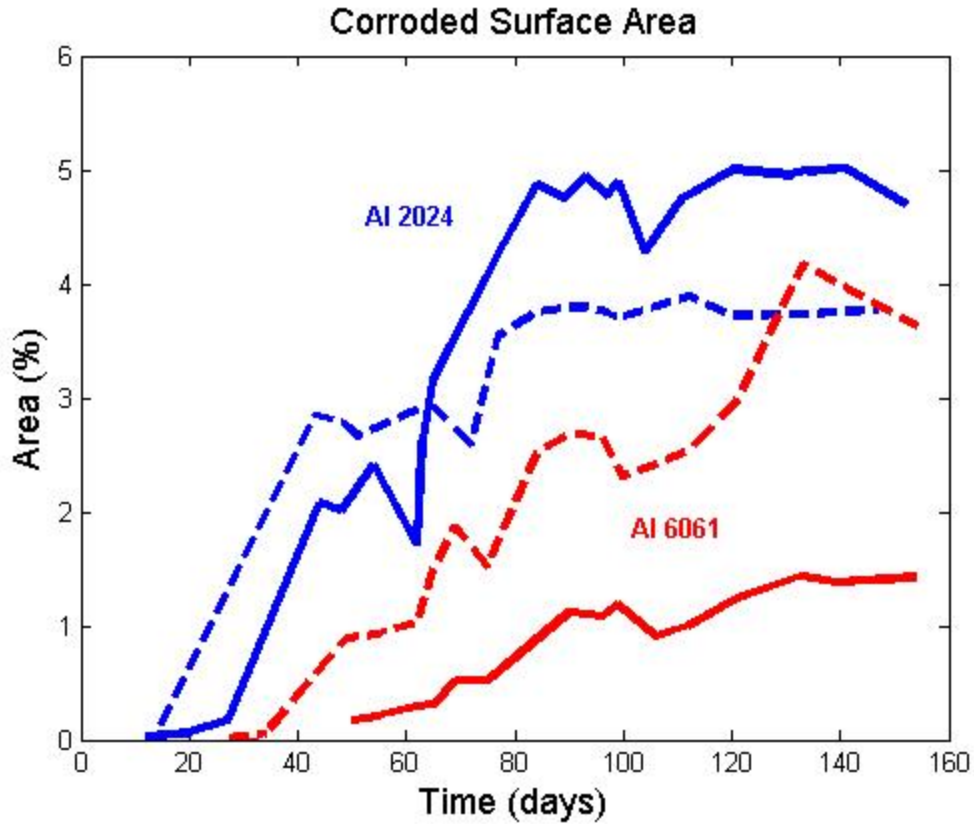


Figure 14: Estimates of corroded surface area over time. Dashed lines are samples in near-stagnant water, solid lines are in 1 m/s flowing water.

### 6.5. CORRODED VOLUME

The total volume of material removed was estimated by calculating the mean corrosion depth over the corroded surface area (Figure 15). These measurements were also normalized based on post-processing profilometer data, but the relative trends are informative and were similar to the corroded surface area and maximum pit depth trends.

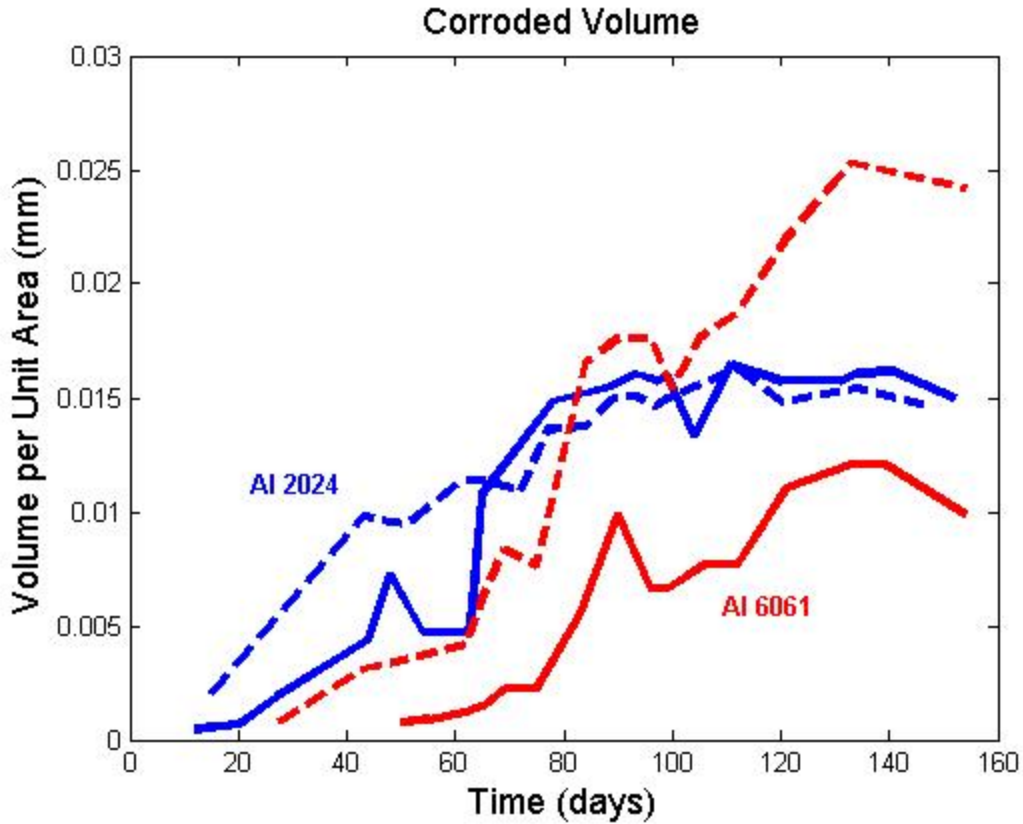
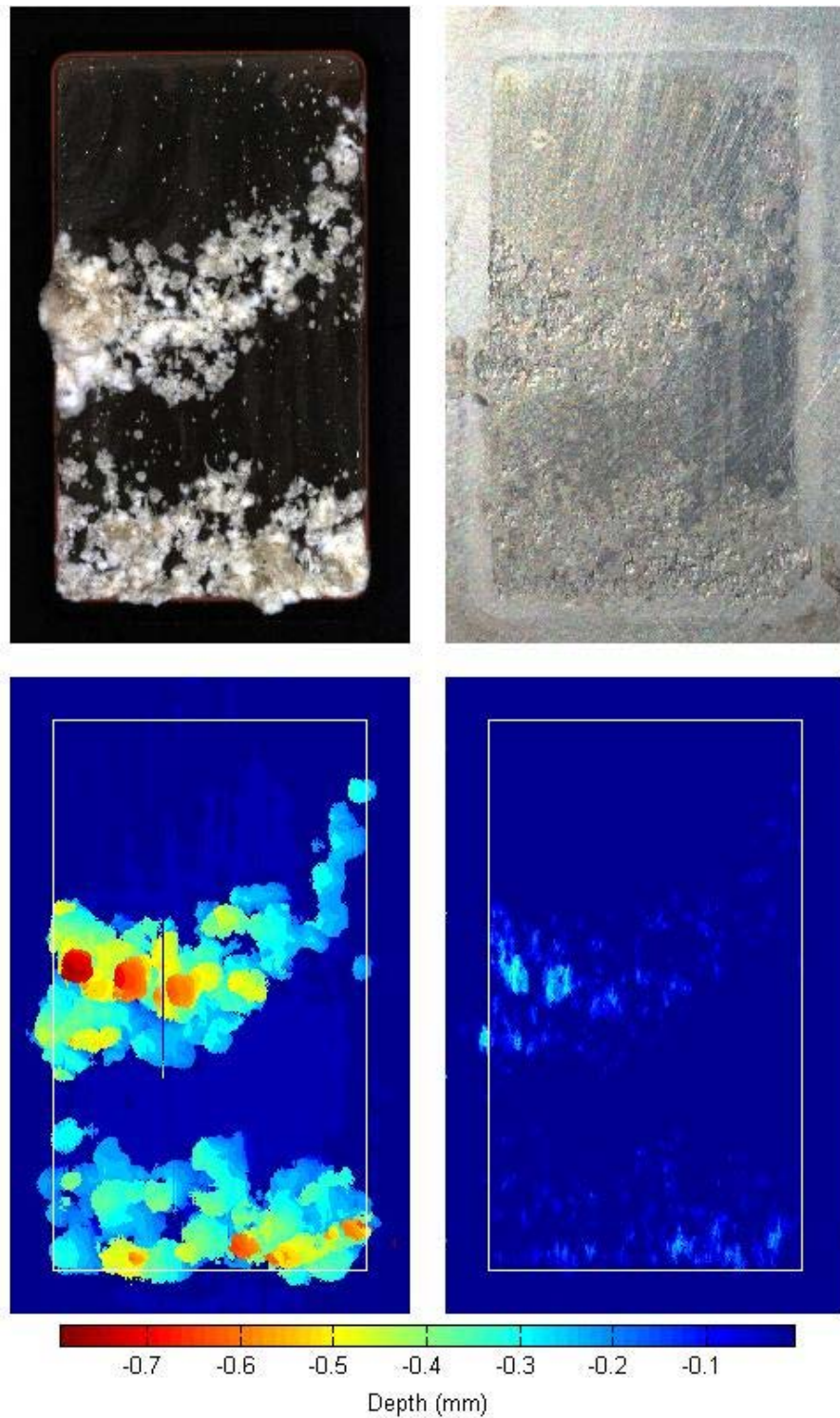


Figure 15: Estimates of total volume of material removed over time. Dashed lines are samples in near-stagnant seawater, solid lines are in 1 m/s flowing seawater.

### 6.6. POST-PROCESSED SAMPLES

Three samples were removed from the experiment for post-processing (Al 2024 from both seawater sources and Al 6061 from the near-stagnant seawater source). The remaining samples continue to be tested to record their long term corrosion development. After removal from seawater, corrosion product was removed from the surface and samples were scanned by the laser profilometer. Figures 16 through 18 compare the different measurement techniques for each removed sample.



*Figure 16: Al 2024 sample in near-stagnant seawater before and after processing. Upper left - surface image while the sample was still in seawater, upper right - sample after corrosion product was removed, lower left - ultrasonic scan performed during testing, lower right - laser profilometer scan after corrosion product was removed. White box shows the location of the gasket's inner edge.*

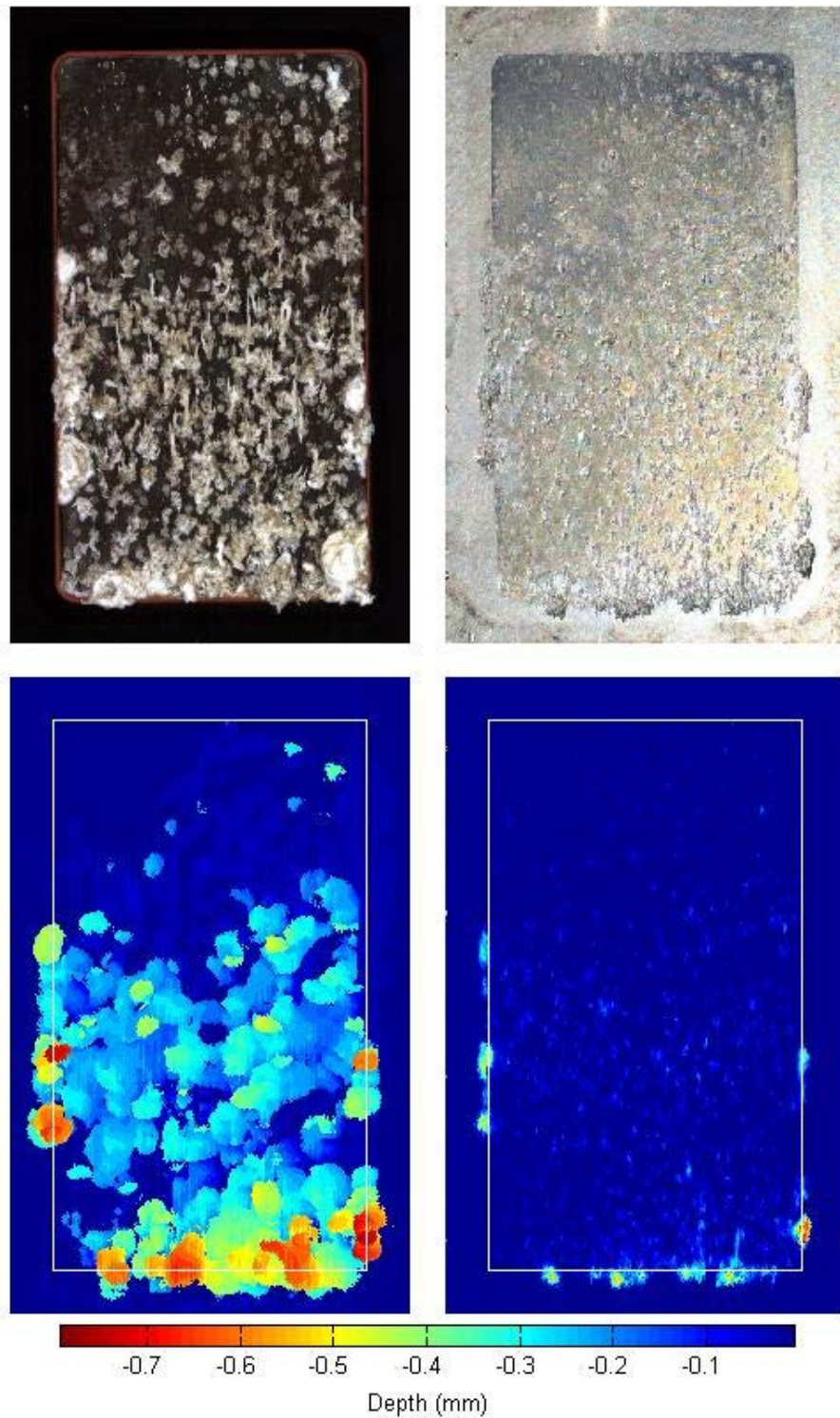


*Figure 17: Al 2024 sample in 1 m/s flowing seawater before and after processing. Upper left - surface image while the sample was still in seawater, upper right - sample after corrosion product was removed, lower left - ultrasonic scan performed during testing, lower right - laser profilometer scan after corrosion product was removed. White box shows the location of the gasket's inner edge.*

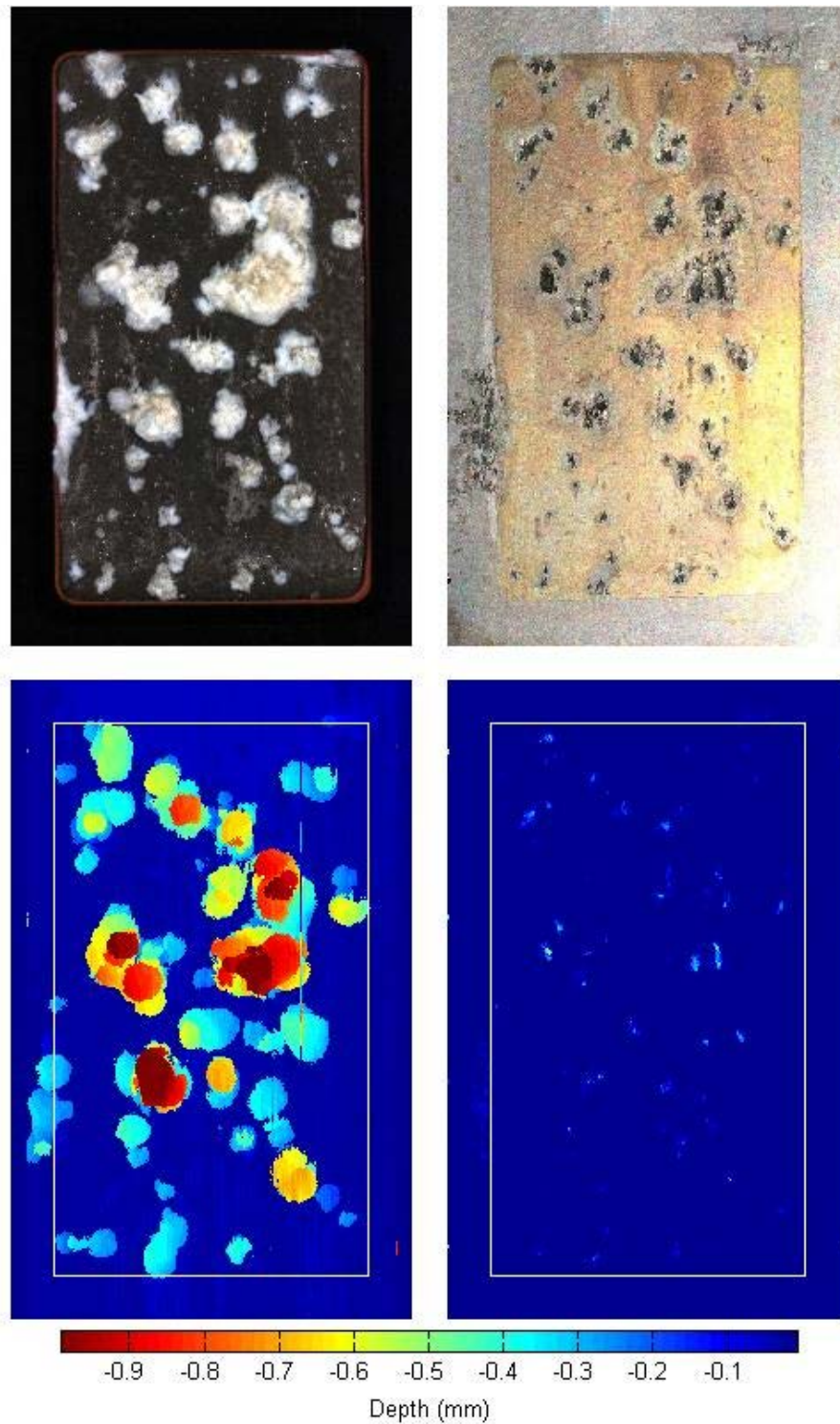


*Figure 18: Al 6061 sample in near-stagnant seawater before and after processing. Upper left - surface image while the sample was still in seawater, upper right - sample after corrosion product was removed, lower left - ultrasonic scan performed during testing, lower right - laser profilometer scan after corrosion product was removed. White box shows the location of the gasket's inner edge.*

The locations of corrosion product accumulation and pitting is strongly correlated. Ultrasonic pits appear wider than pits identified in profilometer scans due to the large transducer beam size. However, there is an unaccounted-for discrepancy between ultrasonically measured and laser profilometry measured pit depths. Profilometry measured pits are shallower than ultrasonically measured pits (Figure 19).

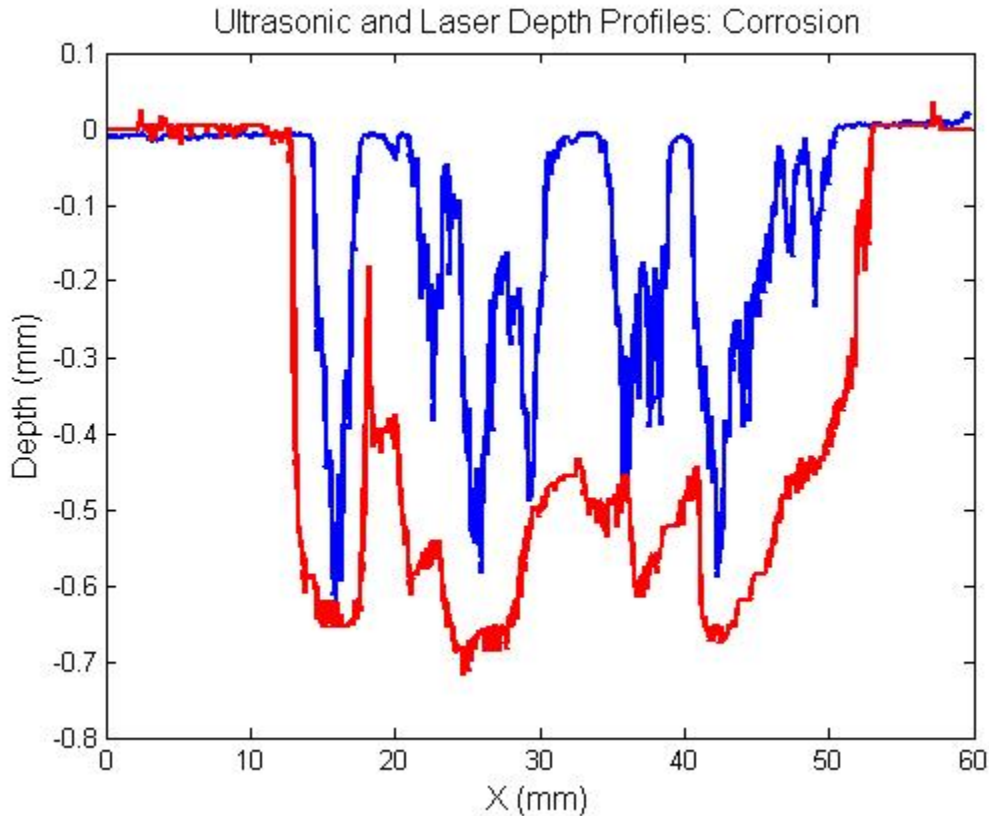


*Figure 19: Corrosion profiles across a sample measured ultrasonically (red) and with the laser profilometer (blue).*

Visual observations show that pits are craterous and porous and can develop undercuts (Figures 20 through 22). Furthermore, the removal of corrosion product can cause changes in the shape of pits as some areas swell and metal fragments that were held in place with corrosion product are removed. Since the profilometer can only measure line-of-sight depths, we hypothesize that inherent pit features obstruct the laser profilometer from measuring the full pit depth. Because the ultrasonic scans pick up the sound reflected from the first surface discontinuity encountered (i.e., the deepest extent of corrosion penetration), the ultrasonic scans are a more conservative measurement of pit growth. Previous pitting studies that used pit depths obtained solely by laser profilometer may have underestimated the extent of pit penetration.

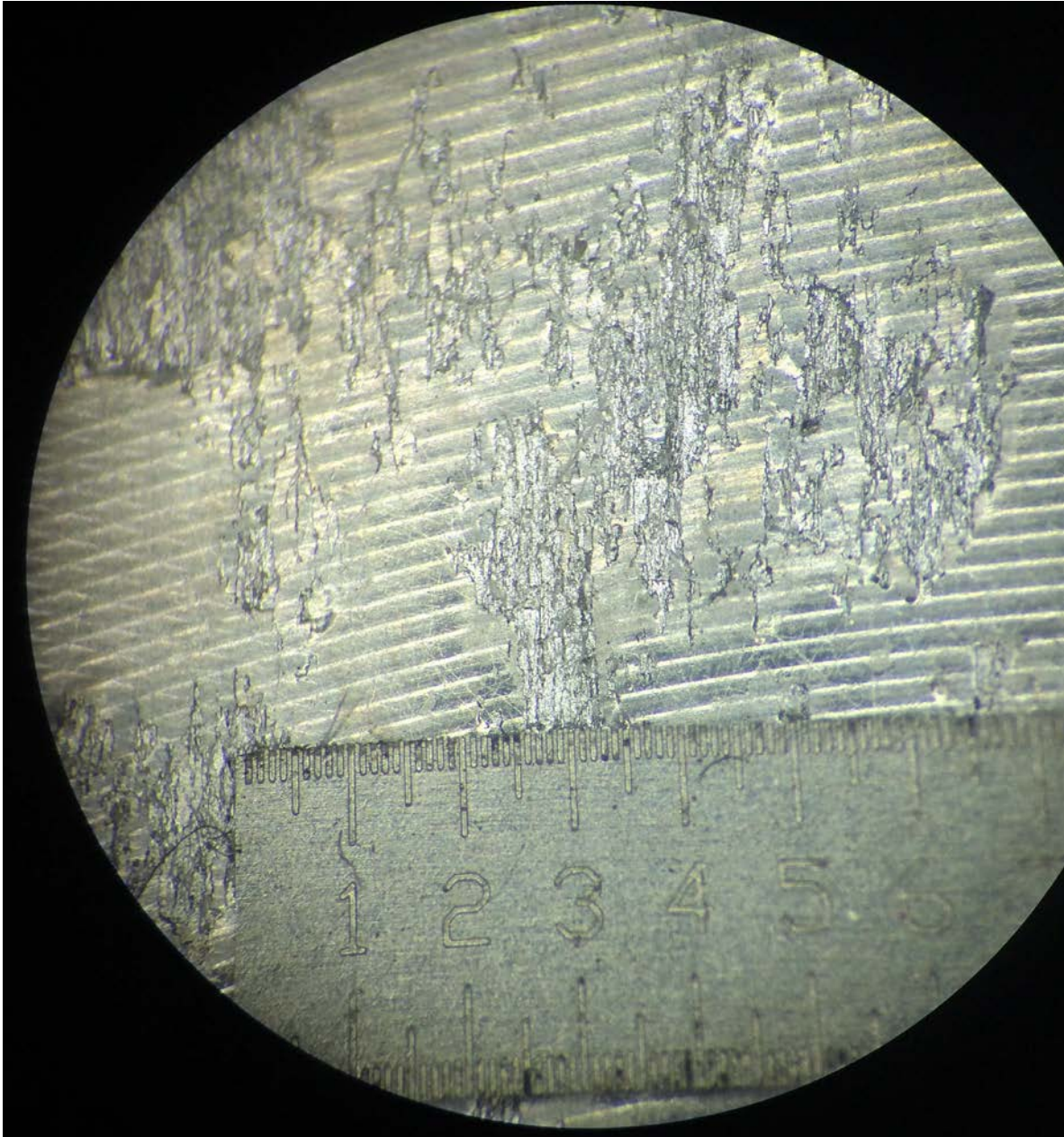


*Figure 20: Pits on the surface of the Al 2024 sample in near-stagnant seawater. Pits are porous and develop preferentially along the extrusion direction.*

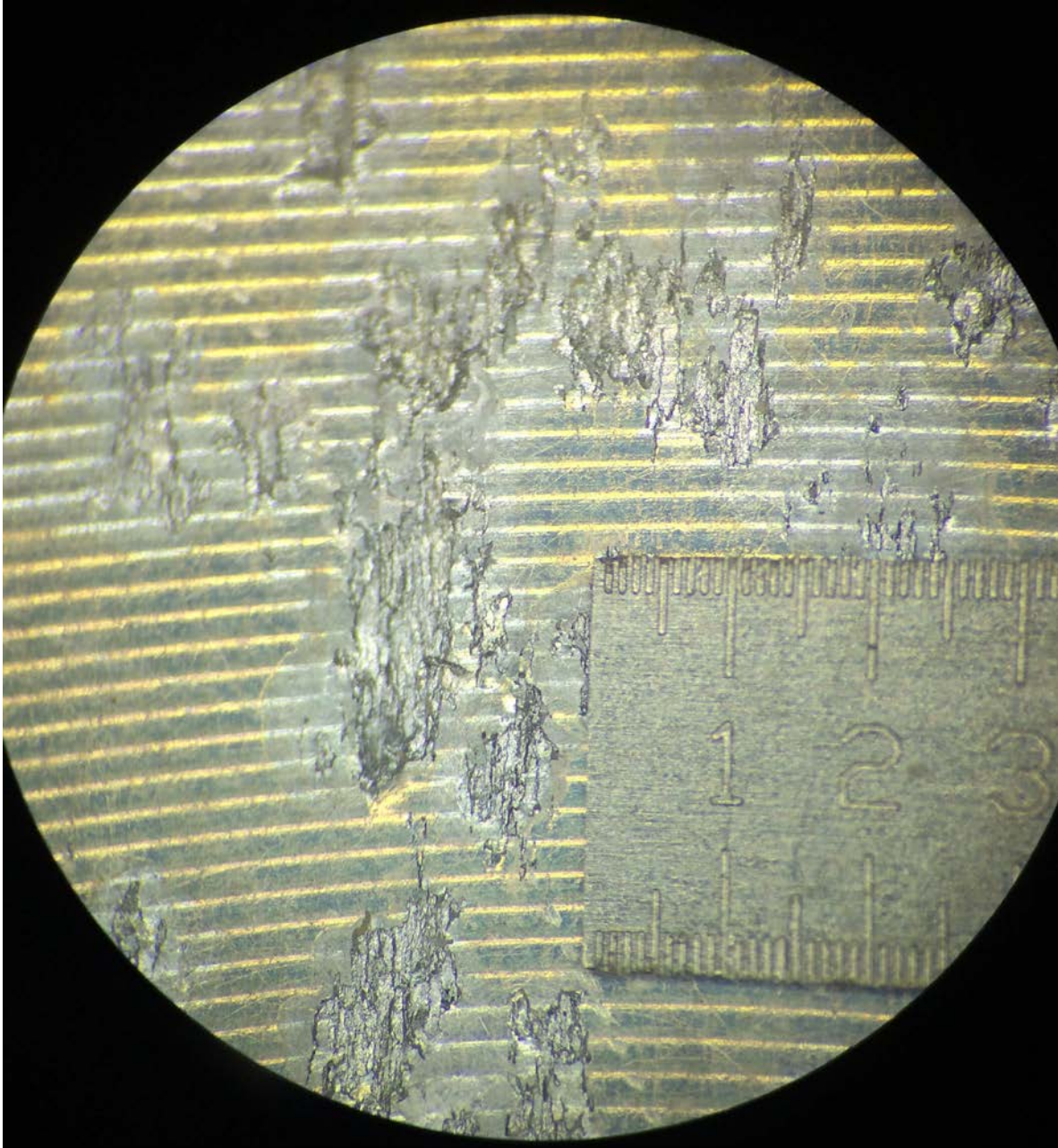


*Figure 21: Pits on the surface of the Al 2024 sample in 1 m/s flowing seawater. Pits are porous and develop preferentially along the extrusion direction.*

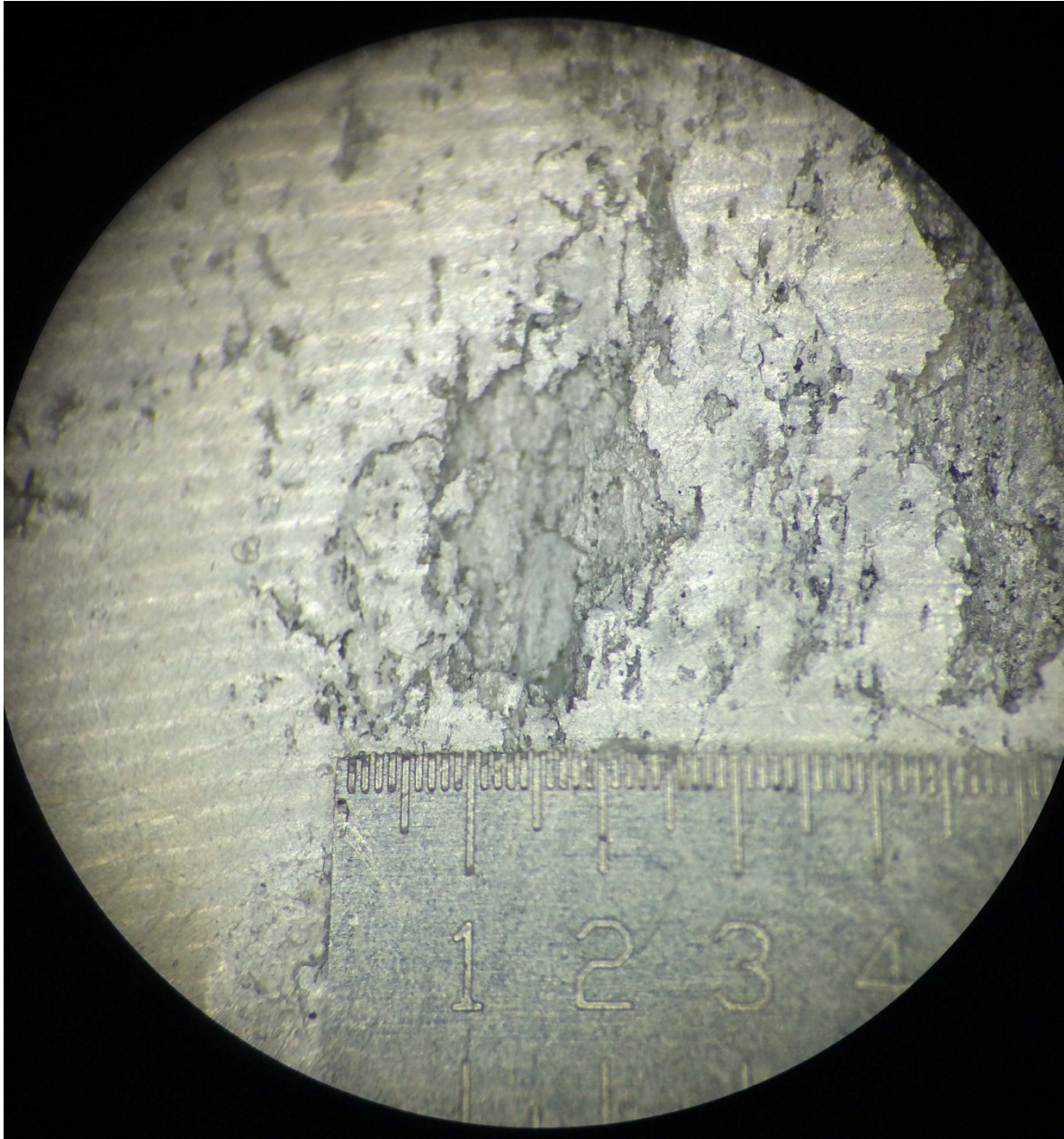


*Figure 22: A pit on the surface of the Al 6061 sample in near-stagnant seawater. Pits are porous and develop preferentially along the extrusion direction.*

#### 6.7. GASKET CREVICE CORROSION

All samples (except Al 5086 in flowing seawater) developed crevice corrosion at the gasket interface (Figures 23 through 25). This form corrosion can slowly open a channel for seawater to leak under the gasket from the heat exchanger into the environment. Although leaks were not observed in any of the samples, the Al 2024 and Al 6061 samples in near-stagnant water developed corrosion outside the gasket, indicating seawater had penetrated under the gasket to the non-exposed side.

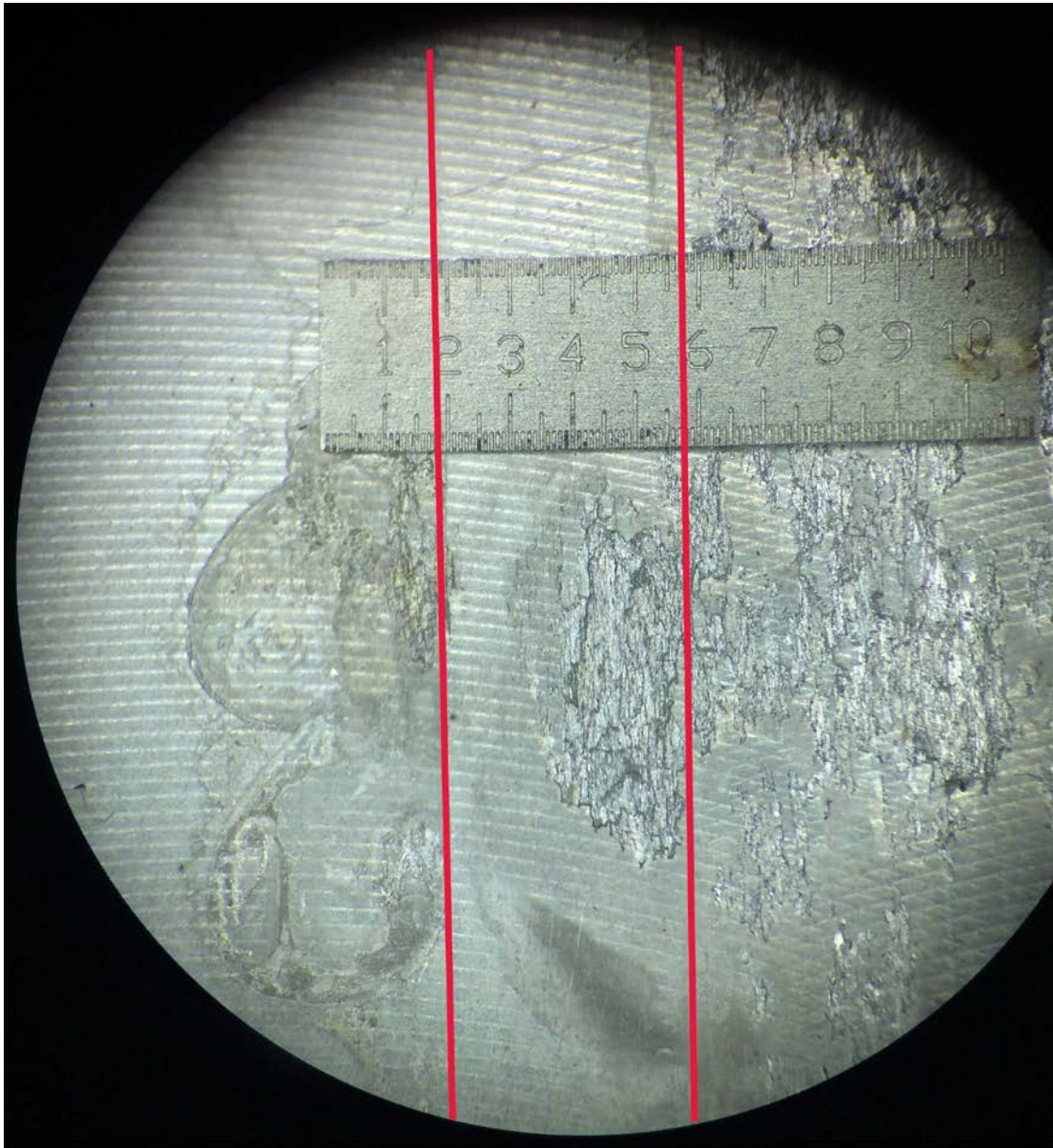


*Figure 23: Corrosion at the gasket (indicated by the red lines) on the Al 2024 sample in near stagnant seawater. Seawater flow is to the right of the gasket and air is to the left. In this sample corrosion has developed outside the gasket, indicating seawater penetration under the gasket.*

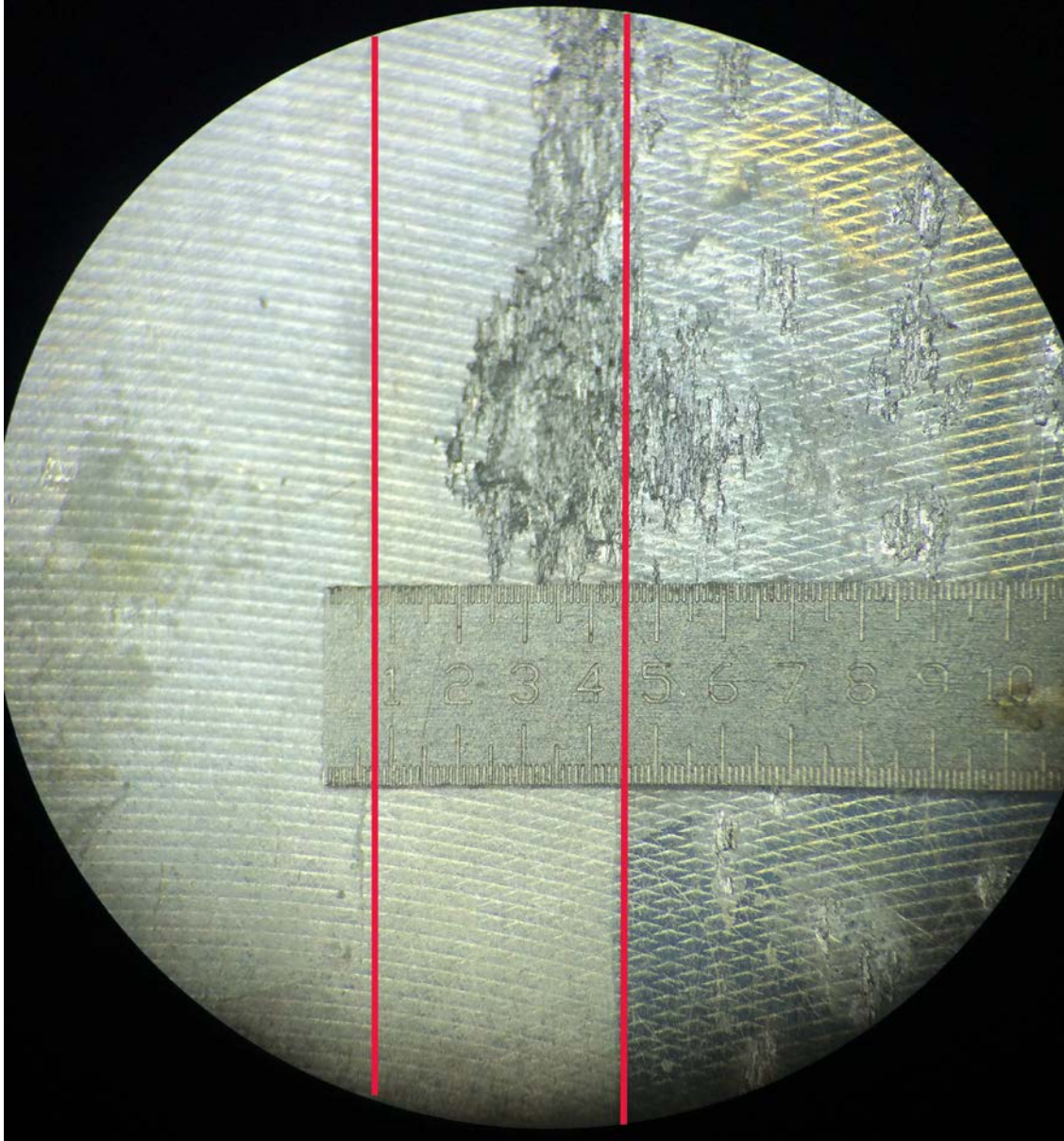


*Figure 24: Corrosion at the gasket (indicated by the red lines) on the Al 2024 sample in 1 m/s flowing seawater. Seawater flow is to the right of the gasket and air is to the left. In this sample there is no indication of seawater penetration under the gasket.*

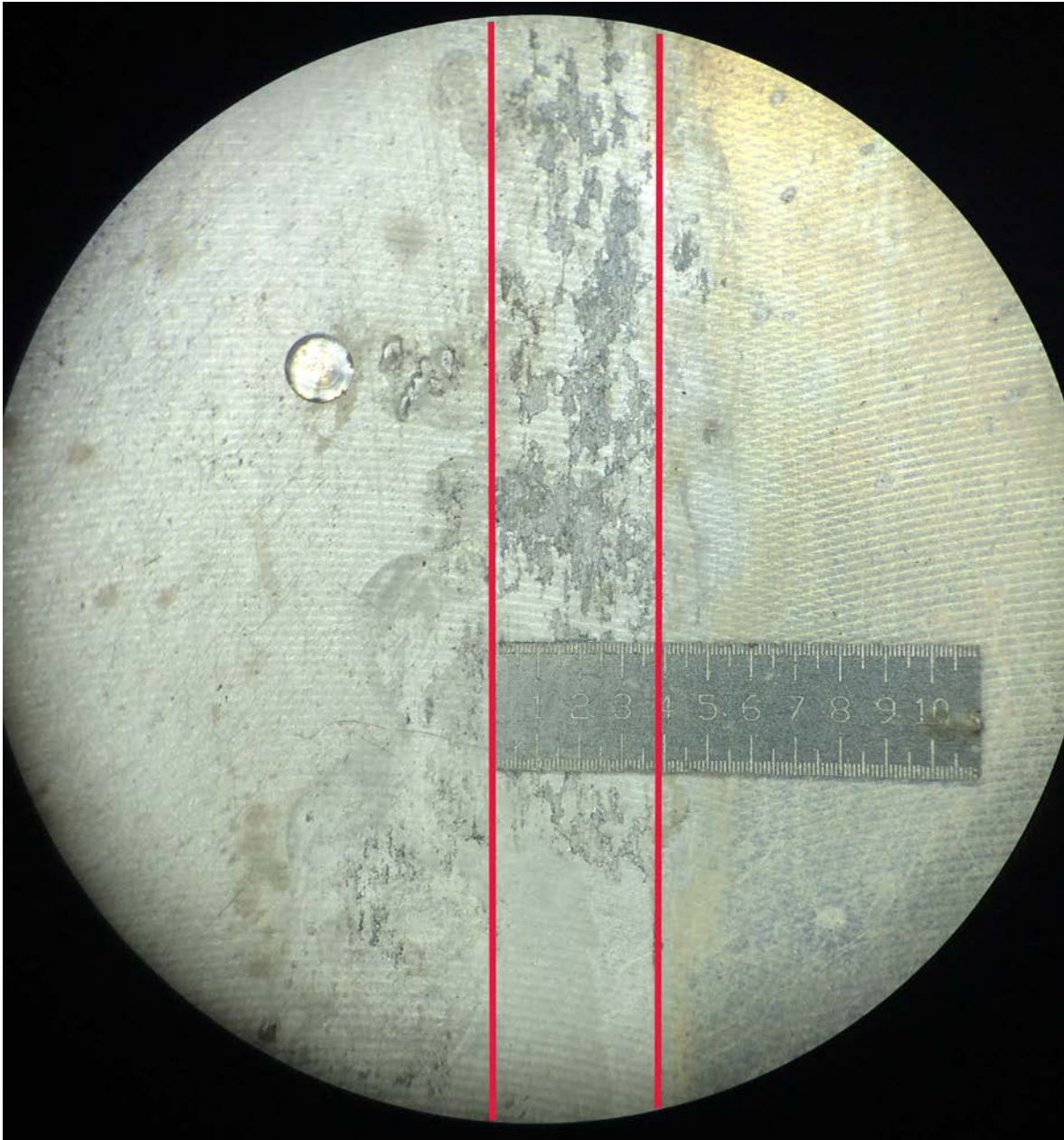


*Figure 25: Corrosion at the gasket (indicated by the red lines) on the Al 6061 sample in 1 m/s flowing seawater. Seawater flow is to the right of the gasket and air is to the left. In this sample corrosion has developed on the outside of the gasket, indicating some degree of seawater penetration under the gasket.*

Lateral gasket corrosion not as catastrophic as pitting corrosion, which would result in working fluid leaking into the seawater. In shell-and-tube heat exchangers, gaskets are located on non-heat transferring surfaces, so a wider gasketed area and thicker base material can compensate for under-gasket corrosion. The extent of seawater penetration under the gasket was measured ultrasonically (Table 4).

Source	Sample	Lateral Penetration from Interior Gasket Edge (mm)	Maximum Corrosion Depth Underneath Gasket (mm)
<b>Near-stagnant Seawater</b>	Al 2024	5	0.6
	Al 6061	6	0.4
	Al 5086	4	0.2
<b>1 m/s Flowing Seawater</b>	Al 2024	3	0.8
	Al 6061	4	0.4
	Al 5086	-	-

*Table 4: Corrosion penetration at the gaskets as determined from ultrasonic scans. Lateral penetration is the distance from the inner edge of the gasket to the furthest extent of detected corrosion.*

#### 6.8. OPEN-CIRCUIT POTENTIALS

Open-circuit potential (OCP) relative to an Ag/AgCl reference electrode was monitored for all samples. OCP is a qualitative indicator of the state of a sample, possibly showing changes indicative of the onset of corrosion. OCP monitoring of OTEC heat exchangers could be a non-destructive technique to identify corrosion development.

OCP of all samples is shown in Figure 26. Al 6061 samples showed a dramatic change in OCP when corrosion product was first observed on the sample, rising abruptly from approximately -1050 mV to approximately -700 mV. OCP of the corroding Al 5086 sample also showed a change in OCP about the time that corrosion was observed, changing from approximately -900 mV to -700 mV. The Al 2024 samples show no dramatic change in OCP upon the appearance of corrosion, but continued to change over time.

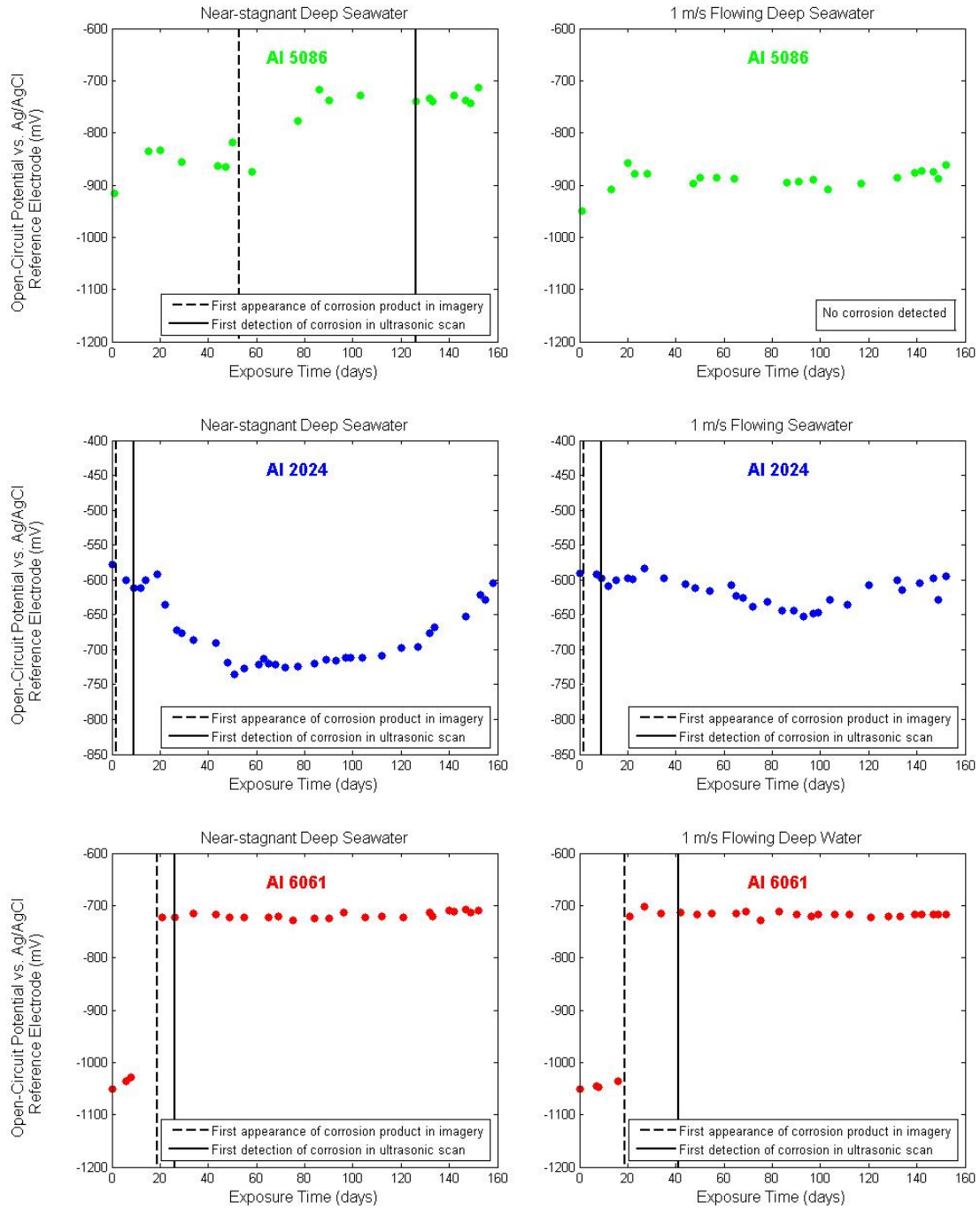


Figure 26: Open-circuit potentials against an Ag/AgCl reference electrode.

## 7. SUMMARY

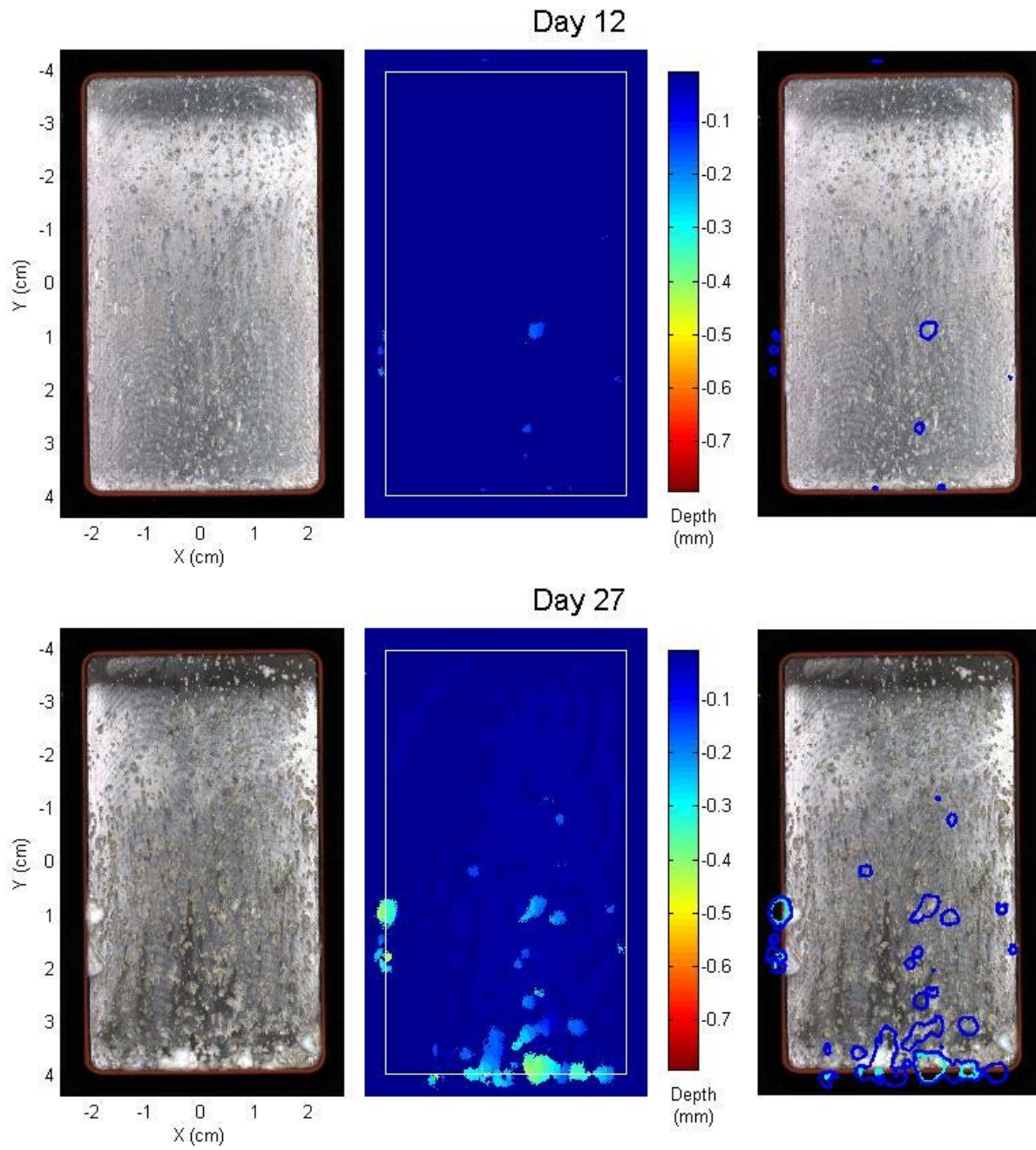
The corrosion development of Al 2024, Al 6061-T651 and Al 5086-H116 in near-stagnant and flowing cold, deep seawater has been observed for 4.5 months. Corrosion development was characterized with three measurement techniques. Ultrasonic scanning is a non-destructive test method that allows measurements of corrosion in-situ without disturbing the samples. Simultaneous in-situ imaging of the corroding surface shows a clear correlation between the accumulation of corrosion product and pitting locations. Post-removal analysis of three samples suggest ultrasonic scanning is superior to laser profilometry in determining the maximum pitting depth because ultrasonic scanning measures the deepest extent of material removal whereas porous pits with undercut caverns can obscure line-of-sight necessary for accurate laser profilometry measurements. As a result, previous measurements of pit depth relying on laser profilometry may be underestimates.

Al 2024 and Al 6061 corroded quickly, developing ~ 1 mm deep pits after several months of exposure to seawater. Both alloys are inappropriate choices for OTEC heat exchangers. Although Al 5086 in flowing seawater has not shown corrosion, crevice corrosion in near-stagnant seawater was observed after 50 days. Corrosion at the gasket interface is not as devastating as corrosion on heat-exchanging surfaces where pits can cause leaks of working fluid into sweater. The effect of crevice corrosion at the gasket interface can be mitigated with proper heat exchanger design. Monitoring of the remaining samples will continue to gather information on the long term development of corrosion on Al 6061 and Al 5086 alloys.

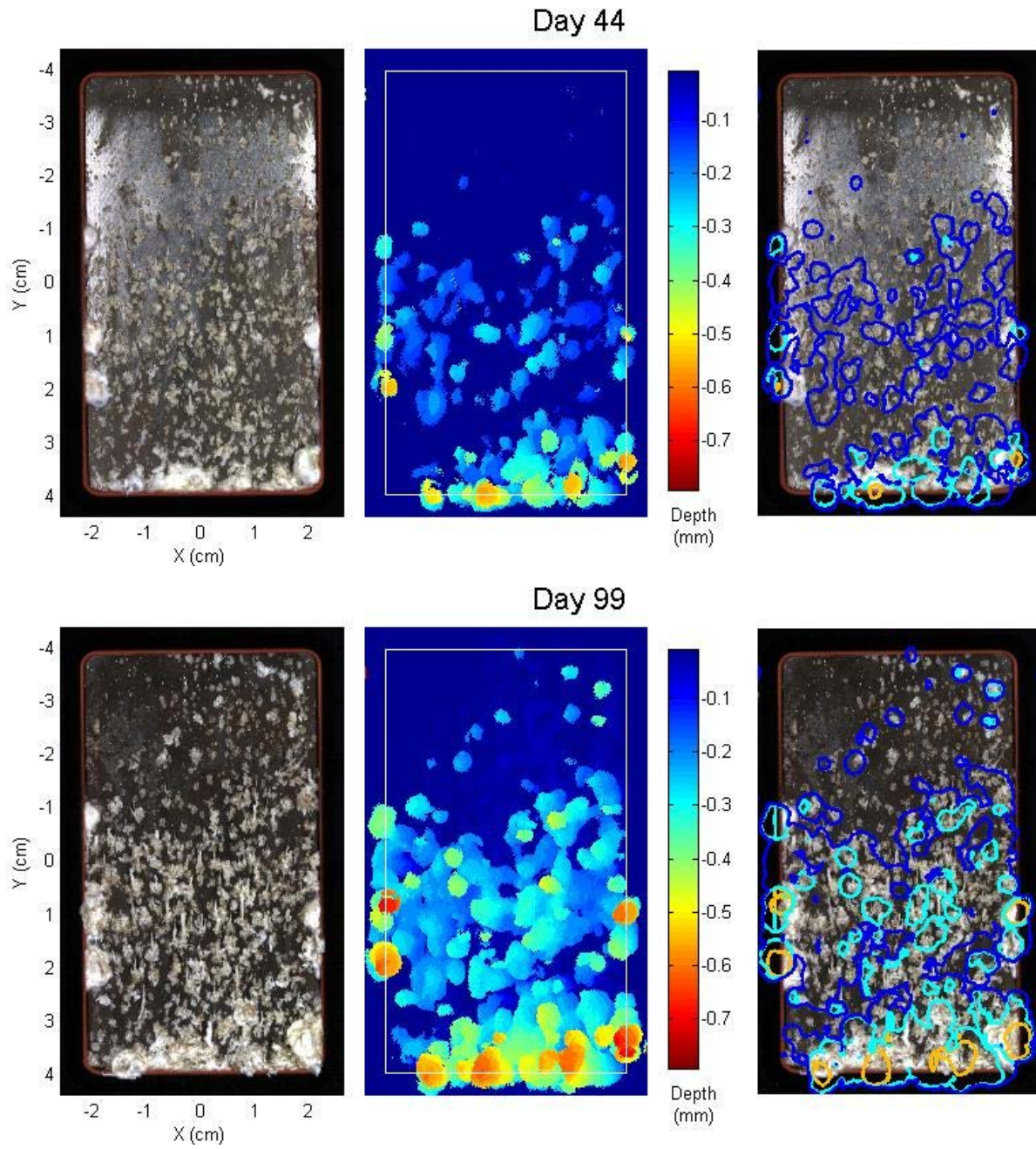
Future work could incorporate ultrasonic scanning into Makai Ocean Engineering's corrosion testing program and focus on aluminum alloys that have demonstrated strong potential for use in OTEC heat exchangers from, as determined by on-going testing. To date, Alloy 3003 has shown the best corrosion resistance in both warm and cold seawater, and could be considered for use in evaporators and condensers. Alloy 5052 has performed well in warm seawater but was susceptible to crevice corrosion in cold seawater. Alloy 6063 has also performed well in warm seawater but was susceptible to pitting in cold seawater. Alloy 5086 is still under consideration for use in both condenser and evaporator with performance similar to Alloy 5052; however, Alloy 5086 has not been tested as long as the other alloys. When considering manufacturing processes, extrusion quality is important; pitting on Alloys 5052 and 6063 were concentrated along extrusion defects. Brazed joints performed poorly in cold seawater and should not be used in a condenser.

Ultrasonic scanning is a powerful means of monitoring corrosion and can be implemented in an OTEC plant. Since the internal surfaces of heat exchangers cannot not be directly scanned, Makai Ocean Engineering recommends that a test apparatus used to expose samples of heat exchanger materials (identical lot and manufacturing processes) under representative seawater conditions (seawater chemistry, flow and pressure) be monitored using ultrasonic scanning techniques. Corrosion development within the functioning heat exchanger could be inferred from sample measurements.

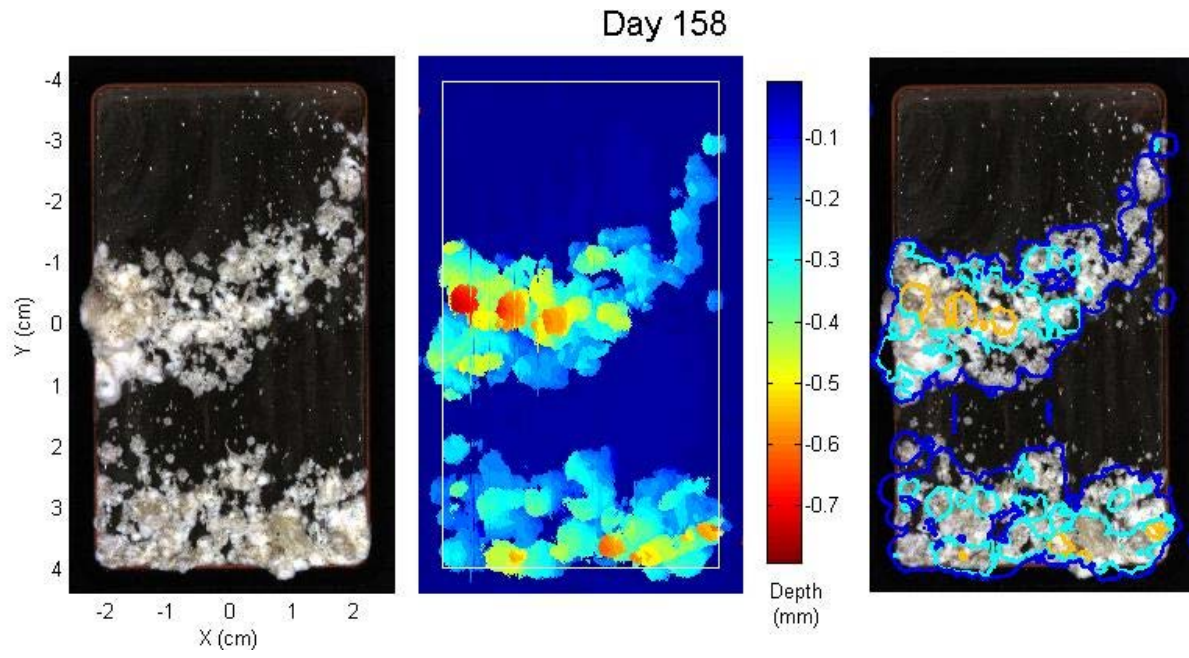
## Appendix A: Al 2024 in flowing 1 m/s seawater.



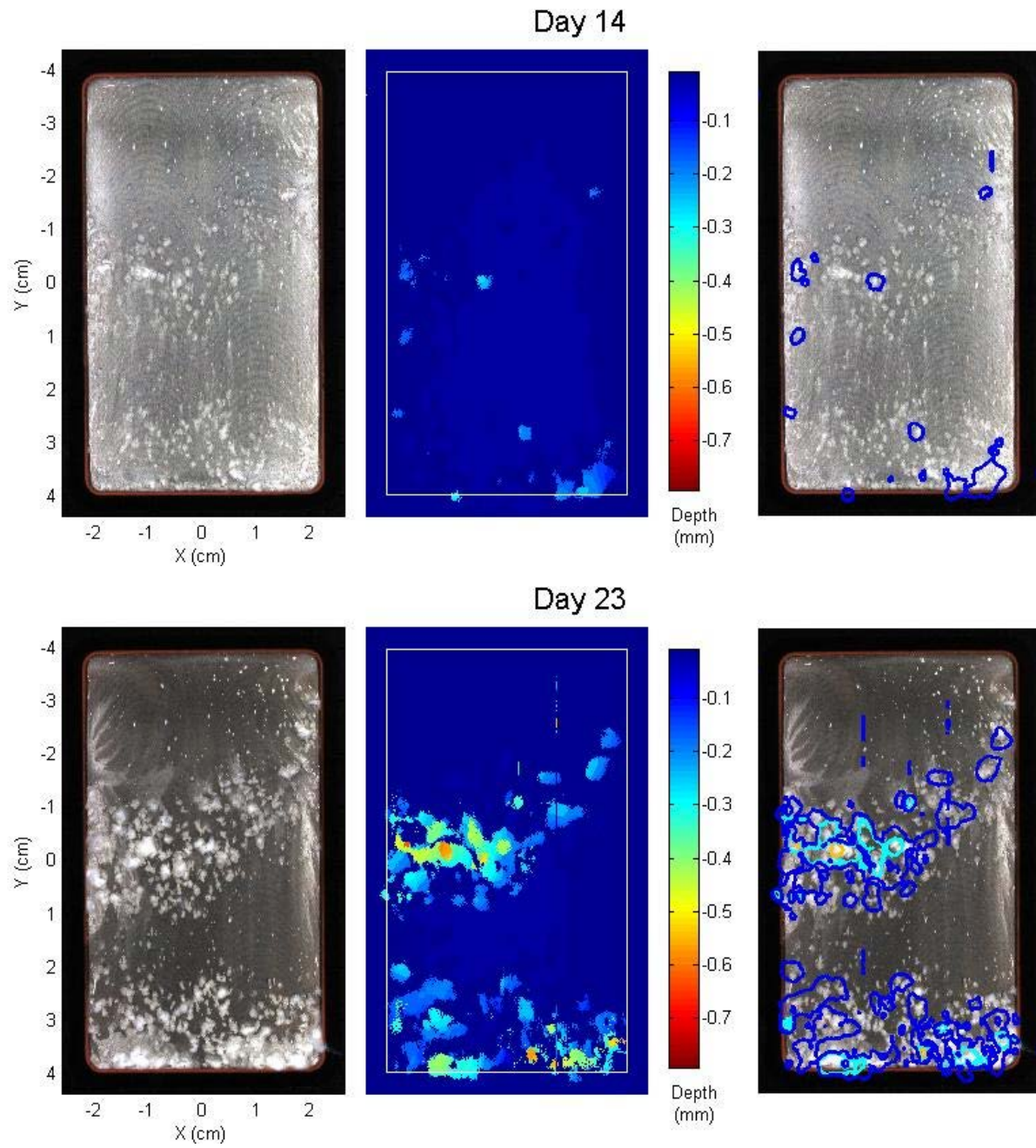
# Appendix A: AI 2024 in flowing 1 m/s seawater.



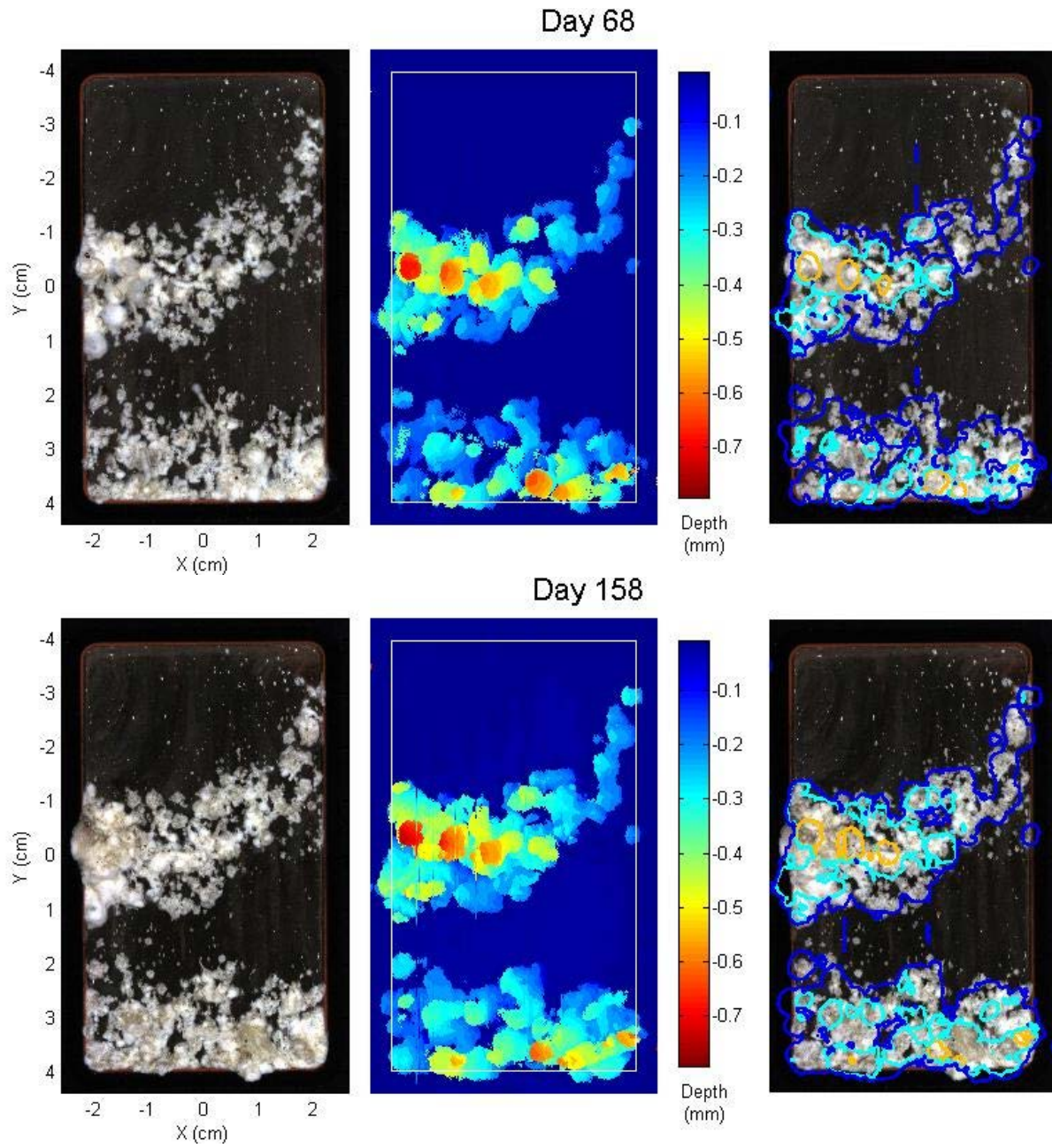
# Appendix A: AI 2024 in flowing 1 m/s seawater.



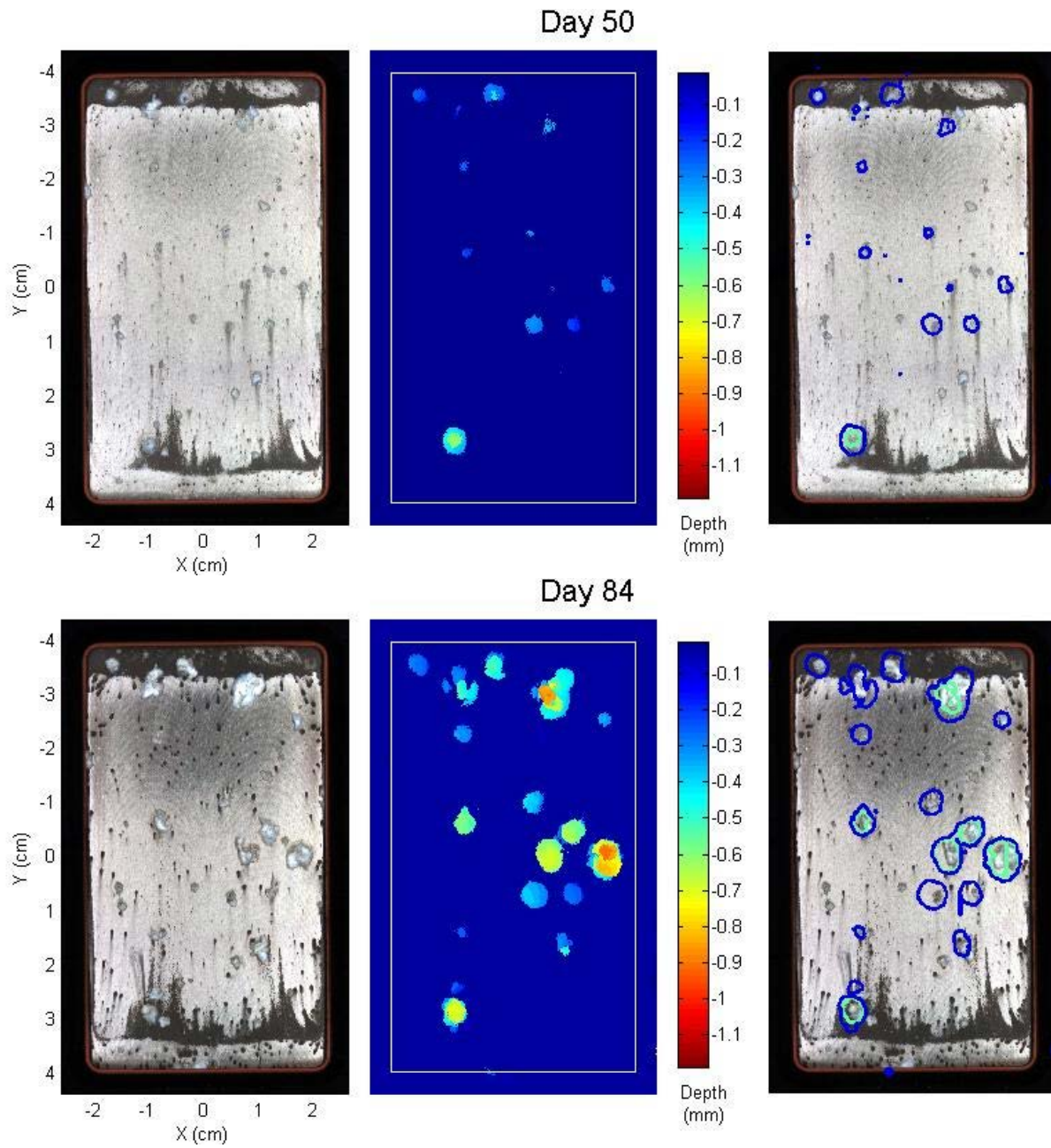
## Appendix B: Al 2024 in near-stagnant seawater.



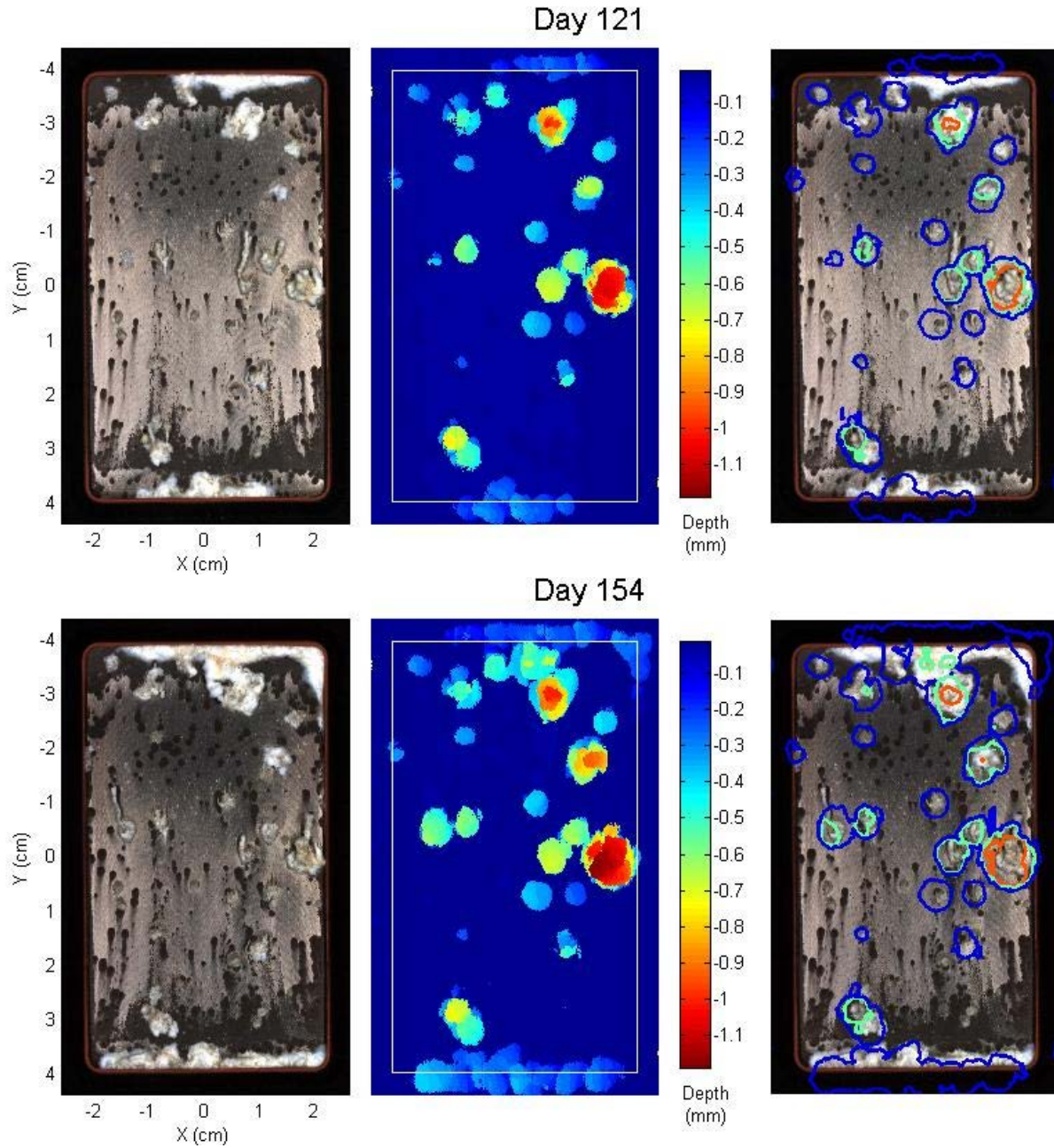
## Appendix B: AI 2024 in near-stagnant seawater.



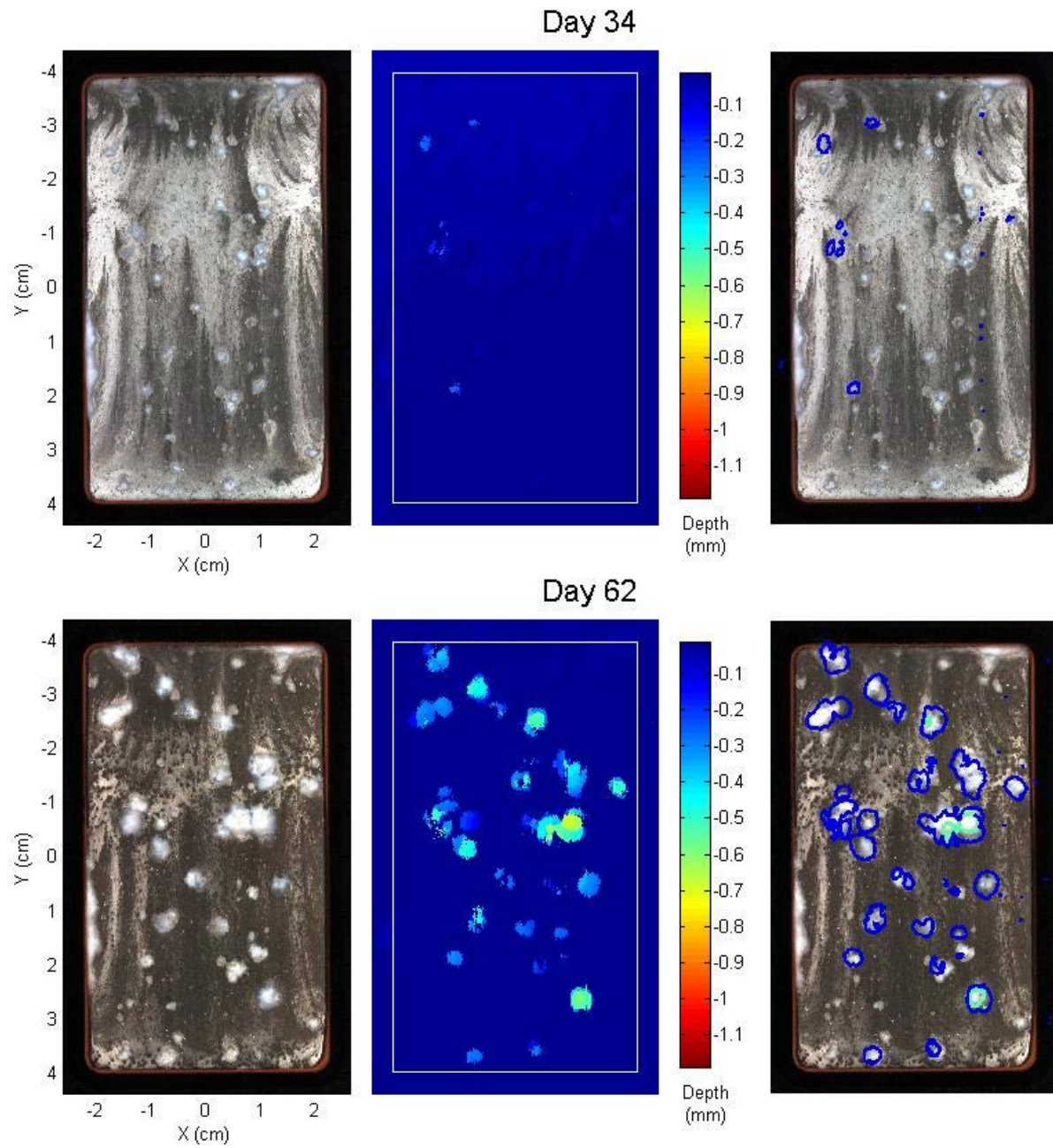
### Appendix C: Al 6061 in flowing 1 m/s seawater.



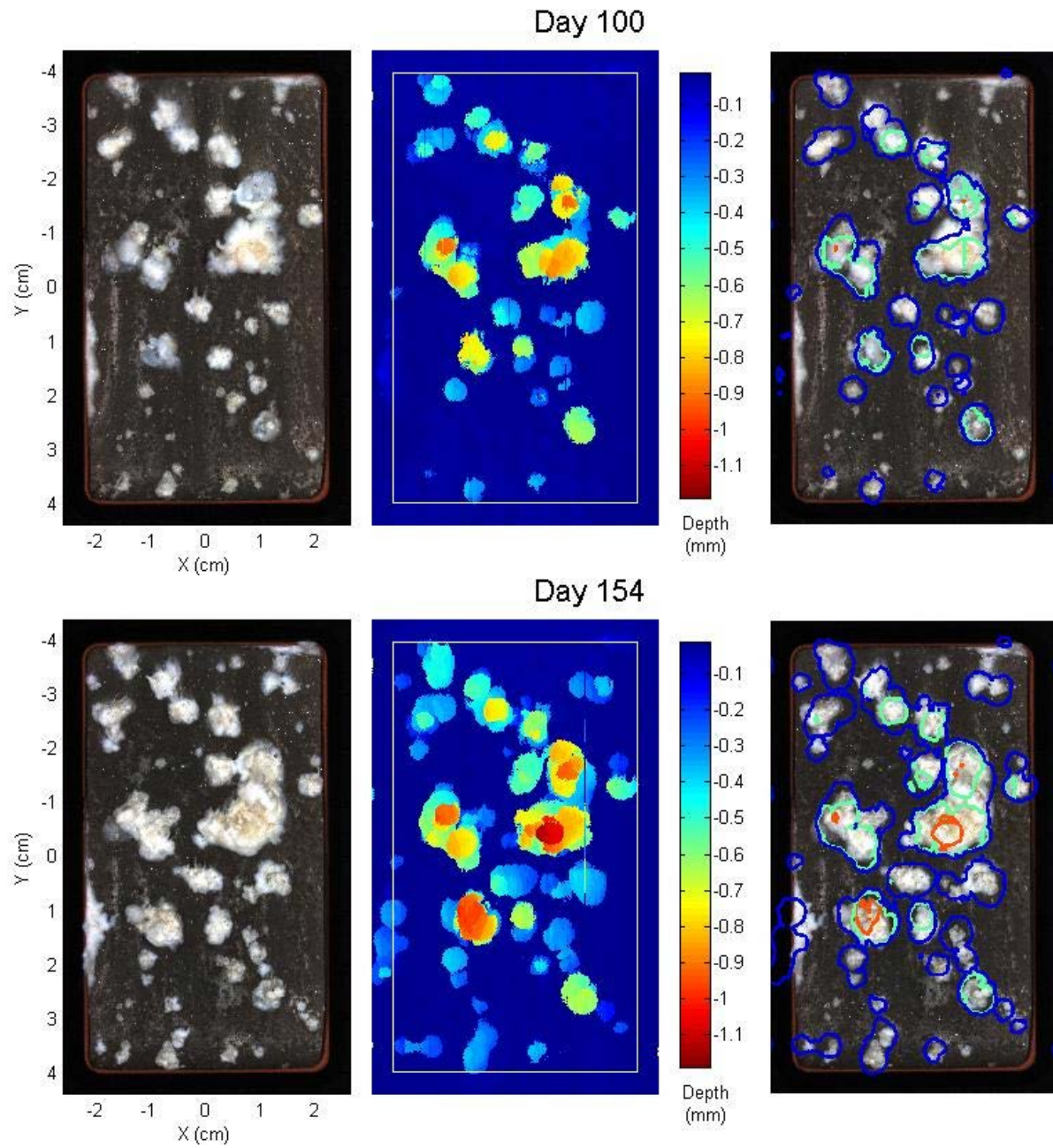
### Appendix C: Al 6061 in flowing 1 m/s seawater.



## Appendix D: Al 6061 in near-stagnant seawater.



## Appendix D: Al 6061 in near-stagnant seawater.



## Appendix E: Al 5086 in near-stagnant seawater.

